



\mathcal{X} -Scene: Large-Scale Driving Scene Generation with High Fidelity and Flexible Controllability

Yu Yang^{1,2} Alan Liang² Jianbiao Mei¹ Yukai Ma¹ Yong Liu¹ Gim Hee Lee²
¹ Zhejiang University ² National University of Singapore
<https://x-scene.github.io/>

Abstract

Diffusion models are advancing autonomous driving by enabling realistic data synthesis, predictive end-to-end planning, and closed-loop simulation, with a primary focus on temporally consistent generation. However, the generation of large-scale 3D scenes that require spatial coherence remains underexplored. In this paper, we propose \mathcal{X} -Scene, a novel framework for large-scale driving scene generation that achieves both geometric intricacy and appearance fidelity, while offering flexible controllability. Specifically, \mathcal{X} -Scene supports multi-granular control, including low-level conditions such as user-provided or text-driven layout for detailed scene composition and high-level semantic guidance such as user-intent and LLM-enriched text prompts for efficient customization. To enhance geometrical and visual fidelity, we introduce a unified pipeline that sequentially generates 3D semantic occupancy and the corresponding multiview images, while ensuring alignment between modalities. Additionally, we extend the generated local region into a large-scale scene through consistency-aware scene outpainting, which extrapolates new occupancy and images conditioned on the previously generated area, enhancing spatial continuity and preserving visual coherence. The resulting scenes are lifted into high-quality 3DGS representations, supporting diverse applications such as scene exploration. Comprehensive experiments demonstrate that \mathcal{X} -Scene significantly advances controllability and fidelity for large-scale driving scene generation, empowering data generation and simulation for autonomous driving.

1 Introduction

Recent advancements in generative AI have profoundly impacted autonomous driving, with diffusion models (DMs) emerging as pivotal tools for data synthesis and driving simulation. Some approaches utilize DMs as data machines, producing high-fidelity driving videos [1–14] or multi-modal synthetic data [15–18] to augment perception tasks, as well as generating corner cases (e.g., vehicle cut-ins) to enrich planning data with uncommon yet critical scenarios. Beyond this, other methods employ DMs as world models to predict future driving states, enabling end-to-end planning [19–21] and closed-loop simulation [22–27]. All these efforts emphasize *long-term video generation through temporal recursion*, encouraging DMs to produce coherent video sequences for downstream tasks.

However, *large-scale scene generation with spatial expansion*, which aims to build expansive and immersive 3D environments for arbitrary driving simulation, remains an emerging yet underexplored direction. A handful of pioneering works have explored 3D driving scene generation at scale. For example, SemCity [28] generates city-scale 3D occupancy grids using DMs, but the lack of appearance details limits its practicality for realistic simulation. UniScene [18] and InfiniCube [29] extend this by generating both 3D occupancy and images, but require a manually defined large-scale layout as a conditioning input, complicating the generation process and hindering flexibility.

In this work, we explore the potential solution to large-scale scene generation with spatial expansion, which faces the following three main challenges: 1) *Flexible Controllability*: Enabling versatile control through both low-level conditions (e.g., layouts) for precise scene composition and high-level prompts (e.g., user-intent text descriptions) for efficient, intuitive customization. For instance, as shown in Fig. 1, users can provide a brief scene description, which the system elaborates into a plausible scene by fully harnessing the generative model’s creative capacity; 2) *High-Fidelity Geometry and Appearance*: generating intricate geometry alongside photorealistic appearance, which is essential to ensure both the structural integrity and visual realism of the 3D scene; 3) *Large-Scale Consistency*: maintaining spatial coherence across interconnected regions to ensure global consistency throughout the extended scene.

To address these challenges, we propose \mathcal{X} -Scene, a novel framework for large-scale driving scene generation. \mathcal{X} -Scene offers: **1) Multi-Granular Controllability**: \mathcal{X} -Scene empowers users to guide generation with varying levels of detail, accommodating both fine-grained layouts for precise control and high-level text prompts for efficient scene customization. To enhance the expressiveness of text-based control, textual prompts are initially enriched by LLMs to form detailed scene narratives. These narratives then inform a text-driven layout generation module that automatically establishes spatial arrangements, guiding subsequent scene synthesis. This dual-control paradigm effectively supports users requiring meticulous, layout-based precision alongside those preferring rapid, prompt-driven customization, thereby broadening accessibility. **2) Geometrical and Visual Fidelity**: \mathcal{X} -Scene achieves high fidelity by employing a unified pipeline that sequentially generates 3D semantic occupancy and the corresponding multiview images. This process ensures both structural accuracy in the 3D geometry and photorealistic visual appearance, promoting inherent consistency and robust alignment between the geometric (occupancy) and visual (image) modalities. **3) Consistent Large-Scale Extrapolation**: To enable the creation of expansive environments, \mathcal{X} -Scene progressively extrapolates new scene content conditioned on adjacent, previously synthesized regions. This consistency-aware outpainting mechanism meticulously preserves spatial continuity, facilitating the seamless and coherent extension of the 3D driving scene well beyond a single local area.

Moreover, to support a diverse array of downstream applications, including realistic driving simulations and immersive free-roam exploration within the generated environments, we further process the synthesized semantic occupancy and multi-view images. Specifically, we reconstruct them into 3D Gaussian (3DGS) [30] representations, a technique adept at faithfully preserving both intricate geometric structures and high-fidelity visual appearance. By unifying these capabilities, \mathcal{X} -Scene advances the state of the art in large-scale, high-fidelity, and controllable driving scene synthesis, empowering data generation and simulation for autonomous driving.

The main contributions of our work are summarized as follows:

- We propose \mathcal{X} -Scene, a novel framework for large-scale 3D driving scene generation with multi-granular controllability, geometrical and visual fidelity, and consistent large-scale extrapolation, supporting a wide range of downstream applications.
- We design a flexible multi-granular control mechanism that synergistically combines high-level semantic guidance (LLM-enriched text prompts) with low-level geometric specifications (user-provided or text-driven layout), enabling scene creation tailored to diverse user needs.
- We present a unified generation and extrapolation pipeline that ensures robust geometric fidelity and photorealistic visual appearance, while also achieving seamless large-scale scene expansion by maintaining spatial and semantic coherence across extrapolated regions.
- Extensive experiments show \mathcal{X} -Scene achieves superior performance in generation quality and controllability, enabling diverse applications from data augmentation to driving simulation.

2 Related Works

2.1 Driving Image and Video Generation

Diffusion models [31–34] have revolutionized image generation by iteratively refining Gaussian noise into high-quality images. Building on this technique, they have significantly advanced autonomous driving by enabling image and video generation for a wide range of downstream applications. For example, several methods synthesize realistic driving images [35, 36, 1] or videos [2–14] from 3D box or layout conditions to support perception tasks through data augmentation. Other approaches [37, 38]

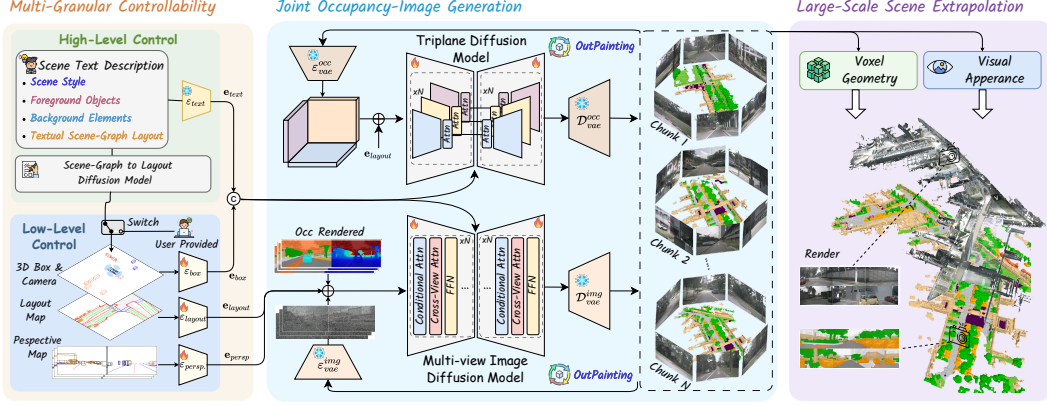


Figure 1: **Pipeline of \mathcal{X} -Scene for scalable driving scene generation:** (a) *Multi-granular controllability* supports both high-level text prompts and low-level geometric constraints for flexible specification; (b) *Joint occupancy-image generation* synthesizes aligned 3D voxels and multi-view images via conditional diffusion; (c) *Large-scale extrapolation* enables coherent scene expansion through consistency-aware outpainting (Fig. 3). Fig. 2 details the scene-graph to layout diffusion.

focus on generating rare yet critical driving events, such as lane changes or vehicle cut-ins, to enhance planning tasks with corner-case scenarios. In addition, some works train diffusion models as world models that predict future driving videos for end-to-end planning [19–21] or closed-loop simulation [22–27]. While existing work predominantly focuses on temporal consistency generation, our work explores the complementary dimension of spatial coherence for large-scale scene generation.

2.2 3D and 4D Driving Scene Generation

Recent advances extend beyond 2D generation to 3D/4D scene synthesis for autonomous driving. These methods generate 3D scenes using various representations, such as LiDAR point clouds [39–44], occupancy volumes [45, 46, 28, 47–50], or 3D Gaussian Splatting (3DGS) [51–53, 38, 54–56], serving as neural simulators for data synthesis and driving simulation. The field has further evolved in two key directions. First, as 3D world models that predict future scene representations—such as point clouds [57–59] or occupancy maps [60–64]—to support planning and pretraining. Second, as multi-modal generators that synthesize aligned cross-modal data, such as image-LiDAR [15, 16] or image-occupancy pairs [17, 18, 24]. In this work, we explore joint occupancy-and-image generation to construct scenes that combine intricate geometry with realistic appearance.

2.3 Large-Scale Scene Generation

Prior work on large-scale city generation has evolved into four main approaches: video-based methods [65, 66], outpainting-based techniques [67–69], PCG-based systems [70–72], and neural-based frameworks [73–75]. While effective at generating natural environments or urban buildings, these methods are not optimized for driving scenarios that require precise street layouts and dynamic agent arrangements. In addition, existing driving-specific solutions face notable limitations. XCube [49] and SemCity [28] generate only geometric occupancy without appearance modeling, while DrivingSphere [24], UniScene [18], and InfiniCube [29] rely on manually defined large-scale layouts, hindering practicality. In contrast, our \mathcal{X} -Scene framework supports joint geometry and appearance generation with flexible, text-based control, enabling more efficient and user-friendly customization.

3 Methodology

\mathcal{X} -Scene strives to generate large-scale 3D driving scenes through a unified framework that addresses controllability, fidelity, and scalability. As illustrated in Fig. 1, \mathcal{X} -Scene comprises three key components: First, the Multi-Granular Controllability module (Sec.3.1) supports both high-level user intent and low-level geometric conditions, enabling flexible scene specification. Next, the Joint Occupancy and Image Generation module (Sec.3.2) leverages conditioned diffusion models to synthesize 3D

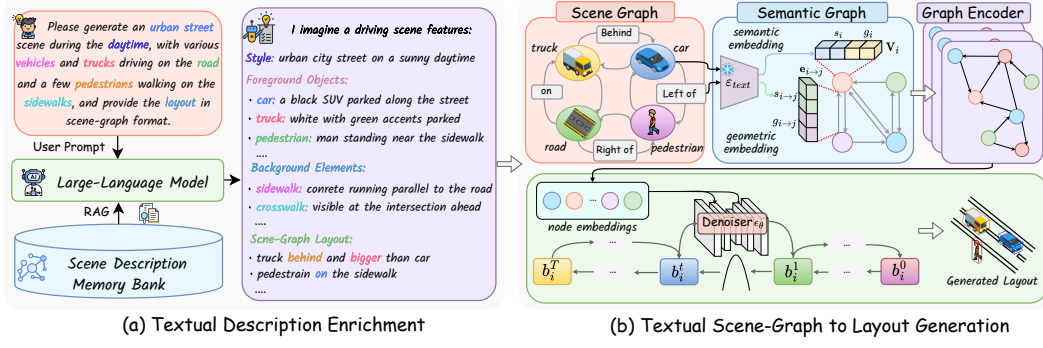


Figure 2: **Pipeline of textual description enrichment and scene-graph to layout generation:** (a) Input prompts are enriched using RAG-augmented LLMs to produce structured scene descriptions; (b) Spatial relationships are converted into a scene graph and encoded with a graph network, followed by conditional diffusion that denoises object boxes and lane polylines into the final layouts.

voxel occupancy and multi-view images, ensuring structural accuracy and photorealistic appearance. Finally, the Large-Scale Scene Extrapolation and Reconstruction module (Sec. 3.3) coherently extends scenes through consistency-aware outpainting and lifts the generated content into 3DGS representations, facilitating downstream simulation and exploration.

3.1 Multi-Granular Controllability

\mathcal{X} -Scene supports dual-mode scene control through: 1) high-level textual prompts, which are enriched by LLMs and converted into structured layouts via a text-to-layout generation model (illustrated in Fig. 2); and 2) direct low-level geometric control for precise spatial specification. This hybrid approach enables both intuitive creative expression and exacting scene customization.

Text Description Enrichment. Given a coarse user-provided textual prompt \mathcal{T}_p , we first enrich it into a comprehensive scene description $\mathcal{D} = \{\mathcal{S}, \mathcal{O}, \mathcal{B}, \mathcal{L}\}$, comprising: scene style \mathcal{S} (weather, lighting, environment), foreground objects \mathcal{O} (semantics, spatial attributes, and appearance), background elements \mathcal{B} (semantics and visual characteristics), and textual scene-graph layout \mathcal{L} , representing spatial relationships among scene entities. The structured description \mathcal{D} is generated as:

$$\mathcal{D} = \mathcal{G}_{\text{description}}(\mathcal{T}_p, \text{RAG}(\mathcal{T}_p, \mathcal{M})) \quad (1)$$

where $\mathcal{M} = \{m_i\}_{i=1}^N$ denotes the scene description memory. Each entity m_i is automatically constructed using one of the N collected scene datasets by: 1) extracting $\{\mathcal{S}, \mathcal{O}, \mathcal{B}\}$ using VLMs on scene images; and 2) converting spatial annotations (object boxes and road lanes) into textual scene-graph layout \mathcal{L} . As shown in Fig. 2, the Retrieval-Augmented Generation (RAG) module retrieves relevant descriptions similar to \mathcal{T}_p from the memory bank \mathcal{M} , which are then composed into a detailed, user-intended scene description by an LLM-based generator $\mathcal{G}_{\text{description}}$.

This pipeline leverages RAG for few-shot retrieval and composition when processing brief user prompts, enabling flexible and context-aware scene synthesis. The memory bank \mathcal{M} is designed to be extensible, allowing seamless integration of new datasets to support a broader variety of scene styles. Additional examples of generated scene descriptions are provided in the appendix.

Textual Scene-Graph to Layout Generation. Given the textual layout \mathcal{L} , we transform it into a detailed layout map through a scene-graph to layout generation pipeline (See Fig. 2). First, we construct a scene graph $\mathcal{G} = (\mathcal{V}, \mathcal{E})$, where nodes $\mathcal{V} = \{v_i\}_{i=1}^M$ represent M scene entities (e.g., cars, pedestrians, road lanes) and edges $\mathcal{E} = \{e_{i \rightarrow j} | i, j \in \{1, \dots, M\}\}$ represent spatial relations (e.g., front of, on top of). Each node and edge is then embedded by concatenating semantic features s_i , $s_{i \rightarrow j}$ (extracted using a text encoder $\mathcal{E}_{\text{text}}$) with learnable geometric embeddings g_i , $g_{i \rightarrow j}$, resulting in node embeddings $\mathbf{v}_i = \text{Concat}(s_i, g_i)$ and edge embeddings $\mathbf{e}_{i \rightarrow j} = \text{Concat}(s_{i \rightarrow j}, g_{i \rightarrow j})$.

The graph embeddings are refined using a graph convolutional network, which propagates contextual information $\mathbf{e}_{i \rightarrow j}$ across the graph and updates each node embedding \mathbf{v}_i via neighborhood aggregation. Finally, layout generation is formulated as a conditional diffusion process: each object layout is

initialized as a noisy 7-D vector $b_i \in \mathbb{R}^7$ (representing box center, dimensions, and orientation), while each road lane begins as a set of N noisy 2D points $p_i \in \mathbb{R}^{N \times 2}$, with denoising process is conditioned on the corresponding node embeddings \mathbf{v}_i to produce geometrically coherent placements.

Low-Level Conditional Encoding. We encode fine-grained conditions (such as user-provided or model-generated layout maps and 3D bounding boxes) into embeddings to enable precise geometric control. As illustrated in Fig. 1, the 2D layout maps are processed by a ConvNet ($\mathcal{E}_{\text{layout}}$) to extract layout embeddings $\mathbf{e}_{\text{layout}}$, while 3D box embeddings \mathbf{e}_{box} are obtained via MLPs (\mathcal{E}_{box}), which fuse object class and spatial coordinate features. To further enhance geometric alignment, we project both the scene layout and 3D boxes into the camera view to generate perspective maps, which are encoded by another ConvNet ($\mathcal{E}_{\text{persp.}}$) to capture spatial constraints from the image plane. Additionally, high-level scene descriptions \mathcal{D} are embedded via a T5 encoder ($\mathcal{E}_{\text{text}}$), providing rich semantic cues for controllable generation through the resulting text embeddings \mathbf{e}_{text} .

3.2 Joint Occupancy and Image Generation

Inspired by [18], we adopt a joint 3D-to-2D generation hierarchy that first models 3D geometry via occupancy diffusion, followed by photorealistic image synthesis guided by occupancy-rendered semantic and depth maps. This 3D-aware guidance ensures geometric consistency and visual realism.

Occupancy Generation via Triplane Diffusion. We adopt a triplane representation [76] to encode 3D occupancy fields with high geometric fidelity. Given an occupancy volume $\mathbf{o} \in \mathbb{R}^{X \times Y \times Z}$, a triplane encoder compresses it into three orthogonal latent planes $\mathbf{h} = \{\mathbf{h}^{xy}, \mathbf{h}^{xz}, \mathbf{h}^{yz}\}$ with spatial downsampling. To mitigate information loss due to reduced resolution, we propose a novel triplane deformable attention mechanism that aggregates richer features for a query point $\mathbf{q} = (x, y, z)$ as:

$$\mathbf{F}_{\mathbf{q}}(x, y, z) = \sum_{\mathcal{P} \in \{xy, xz, yz\}} \sum_{k=1}^K \sigma(\mathbf{W}_{\omega}^{\mathcal{P}} \cdot \text{PE}(x, y, z))_k \cdot \mathbf{h}^{\mathcal{P}}(\text{proj}_{\mathcal{P}}(x, y, z) + \Delta p_k^{\mathcal{P}}) \quad (2)$$

where K is the number of sampling points, $\text{PE}(\cdot) : \mathbb{R}^3 \rightarrow \mathbb{R}^D$ denotes positional encoding, and $\mathbf{W}_{\omega}^{\mathcal{P}} \in \mathbb{R}^{K \times D}$ generates attention weights with the softmax function $\sigma(\cdot)$. The projection function $\text{proj}_{\mathcal{P}}$ maps 3D coordinates to 2D planes (e.g., $\text{proj}_{xy}(x, y, z) = (x, y)$), and the learnable offset $\Delta p_k^{\mathcal{P}} = \mathbf{W}_o^{\mathcal{P}}[k] \cdot \text{PE}(x, y, z) \in \mathbb{R}^2$ uses weights $\mathbf{W}_o^{\mathcal{P}} \in \mathbb{R}^{2 \times D}$ to shift sampling positions for better feature alignment. Then the triplane-VAE decoder reconstructs the 3D occupancy field from the aggregated features $\mathbf{F}_{\mathbf{q}}$.

Building on the latent triplane representation \mathbf{h} , we introduce a conditional diffusion model $\epsilon_{\theta}^{\text{occ}}$ that synthesizes novel triplanes through iterative denoising. At each timestep t , the model refines a noisy triplane \mathbf{h}_t toward the clean target \mathbf{h}_0 using two complementary conditioning strategies: 1) additive spatial conditioning with the layout embedding $\mathbf{e}_{\text{layout}}$; and 2) cross-attention-based conditioning with $\mathcal{C} = \text{Concat}(\mathbf{e}_{\text{box}}, \mathbf{e}_{\text{text}})$, integrating geometric and semantic constraints. The model is trained to predict the added noise ϵ using the denoising objective: $\mathcal{L}_{\text{diff}}^{\text{occ}} = \mathbb{E}_{t, \mathbf{h}_0, \epsilon} [\|\epsilon - \epsilon_{\theta}^{\text{occ}}(\mathbf{h}_t, t, \mathbf{e}_{\text{layout}}, \mathcal{C})\|_2^2]$.

Image Generation with 3D Geometry Guidance. After obtaining the 3D occupancy, we convert voxels into 3D Gaussian primitives parameterized by voxel coordinates, semantics, and opacity, which are rendered into semantic and depth maps via tile-based rasterization [30]. To further incorporate object-level geometry, we generate normalized 3D coordinates for the entire scene and use object bounding boxes to extract relevant coordinates, which are encoded into object positional embeddings \mathbf{e}_{pos} to provide fine-grained geometric guidance. The semantic, depth, and perspective maps are processed by ConvNets and fused with \mathbf{e}_{pos} to form the final geometric embedding \mathbf{e}_{geo} . This embedding is then combined with noisy image latents to enable pixel-aligned geometric guidance. The image diffusion model $\epsilon_{\theta}^{\text{img}}$ further leverages cross-attention with conditions \mathcal{C} (text, camera, and box embeddings) for appearance control. The model is trained via: $\mathcal{L}_{\text{diff}}^{\text{img}} = \mathbb{E}_{t, \mathbf{x}_0, \epsilon} [\|\epsilon - \epsilon_{\theta}^{\text{img}}(\mathbf{x}_t, t, \mathbf{e}_{\text{geo}}, \mathcal{C})\|_2^2]$.

3.3 Large-Scale Scene Extrapolation and Reconstruction

Building on our single-chunk scene generation, we propose a progressive extrapolation approach that coherently expands occupancy and images across multiple chunks, and reconstructs them into an amodal 3DGS with integrated geometry and appearance for versatile downstream applications.

Geometry-Consistent Scene Outpainting. We extend the occupancy field via triplane extrapolation [77], which decomposes the task into extrapolating three orthogonal 2D planes, as illustrated in Fig. 3. The core idea is to generate a new latent plane $\mathbf{h}_0^{\text{new}}$ by synchronizing its denoising process with the forward diffusion of a known reference plane $\mathbf{h}_0^{\text{ref}}$, guided by an overlap mask \mathbf{M} . Specifically, at each denoising step t , the new latent is updated as:

$$\mathbf{h}_{t-1}^{\text{new}} \leftarrow (\sqrt{\bar{\alpha}_t} \mathbf{h}_0^{\text{ref}} + \sqrt{1 - \bar{\alpha}_t} \epsilon) \odot \mathbf{M} + \epsilon_{\theta}^{\text{occ}}(\mathbf{h}_t^{\text{new}}, t) \odot (1 - \mathbf{M}) \quad (3)$$

where $\epsilon \sim \mathcal{N}(\mathbf{0}, \mathbf{I})$ and $\bar{\alpha}_t$ is determined by the noise scheduler at timestep t . This method allows the new latent to preserve structural consistency in the overlapped region while plausibly extending the reference content into unseen areas, resulting in coherent and geometry-consistent scene extensions.

Visual-Coherent Image Extrapolation.

Beyond occupancy outpainting, we further extrapolate the image field for synchronized appearance generation. To ensure visual coherence in the overlapped region between the reference image $\mathbf{x}_0^{\text{ref}}$ and the new view $\mathbf{x}_0^{\text{new}}$, a naive solution warps $\mathbf{x}_0^{\text{ref}}$ using the camera pose (R, T) and applies image inpainting (see Fig. 3). However, solely using the warped images as conditions is insufficient. To overcome this, we fine-tune the diffusion model $\epsilon_{\theta}^{\text{img}}$ with explicit conditioning on $\mathbf{x}_0^{\text{ref}}$ and camera embeddings $\mathbf{e}(R, T)$. Specifically, $\mathbf{x}_0^{\text{ref}}$ is concatenated with the noisy novel image $\mathbf{x}_t^{\text{new}}$, while $\mathbf{e}(R, T)$ is injected via cross-attention. This enables view-consistent extrapolation while retaining photorealistic generation.

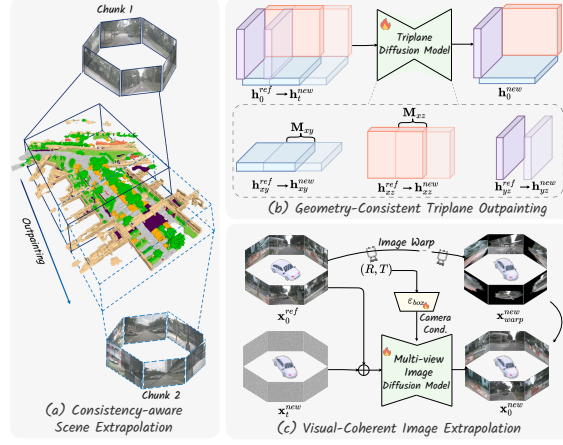


Figure 3: **Illustration of consistency-aware outpainting:** (a) Occupancy triplane extrapolation is decomposed into the extrapolation of three 2D planes, guided by priors from overlapping regions; (b) Image extrapolation is performed via diffusion conditioned on images and camera parameters.

4 Experiments

4.1 Experimental Settings

We use Occ3D-nuScenes[78] to train our occupancy generation module and nuScenes[79] for the multi-view image generation module. Additional implementation details are provided in the appendix.

Experimental Tasks and Metrics. We evaluate \mathcal{X} -Scene across three aspects using a range of metrics: **1) Occupancy Generation:** We evaluate the reconstruction results of the VAE with IoU and mIoU metrics. For occupancy generation, following [50], we report both generative 3D and 2D metrics, including Inception Score, FID, KID, Precision, Recall, and F-Score. **2) Multi-view Image Generation:** We evaluate the quality of the synthesized images using FID. **3) Downstream Tasks:** We evaluate the sim-to-real gap by measuring performance on the generated scenes across downstream tasks, including semantic occupancy prediction (IoU and mIoU), 3D object detection (mAP and NDS), and BEV segmentation (mIoU for the road and vehicle classes).

4.2 Qualitative Results

Large-Scale Scene Generation. The upper part of Figure 4 presents the large-scale scene generation results. By iteratively applying consistency-aware outpainting, \mathcal{X} -Scene effectively extends local regions into coherent and large-scale driving scenes. Furthermore, the generated scenes can be reconstructed into 3D representations, enabling novel view synthesis and supporting downstream perception tasks. Please refer to the Appendix for additional qualitative results.

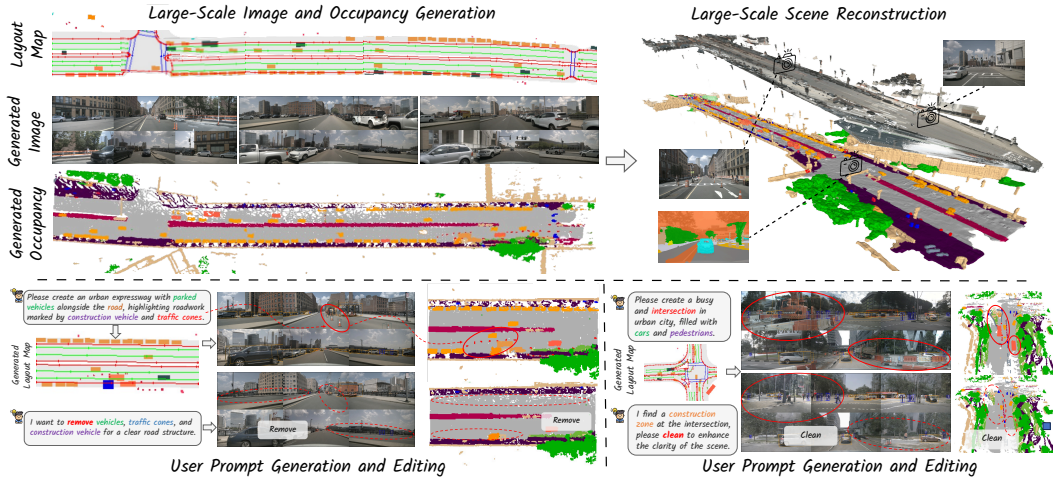


Figure 4: **Versatile generation capability of \mathcal{X} -Scene**: (a) Generation of large-scale, consistent semantic occupancy and multi-view images, which are reconstructed into 3D scenes for novel view rendering; (b) User-prompted layout and scene generation, along with scene geometry editing.

Table 1: **Comparisons of occupancy reconstruction of the VAE**. The downsampled size is reported in terms of spatial dimensions (H, W) and feature dimension (C).

| Method | OccSora [61] (VQVAE) | OccWorld [60] (VQVAE) | OccLLama [80] (VQVAE) | UniScene [18] (VAE) | \mathcal{X} -Scene (Ours) (Triplane-VAE) |
|-----------------------------------|-------------------------|--------------------------|--------------------------|------------------------|---|
| Downsampled Size | (T/8,25,25,512) | (50,50,128) | (50,50,128) | (50,50,8) | (50,50,8) (100,100,16) |
| mIoU \uparrow | 27.4 | 66.4 | 65.9 | 72.9 | 73.7 92.4 |
| IoU \uparrow | 37.0 | 62.3 | 57.7 | 64.1 | 65.1 85.6 |

Table 2: **Comparisons of 3D Occupancy Generation**. We report Inception Score (IS), Fréchet Inception Distance (FID), Kernel Inception Distance (KID), Precision (P), Recall (R), and F-Score (F) in both the **2D** and **3D** domains. \dagger denotes unconditioned generation, while other methods are evaluated using layout conditions. All methods are implemented using official codes and checkpoints.

| Method | #Classes | Metric ^{2D} | | | | | | Metric ^{3D} | | | | | |
|--|----------|-----------------------------|--------------------------------|--------------------------------|----------------------------|----------------------------|----------------------------|-----------------------------|--------------------------------|--------------------------------|----------------------------|----------------------------|----------------------------|
| | | IS ^{2D} \uparrow | FID ^{2D} \downarrow | KID ^{2D} \downarrow | P ^{2D} \uparrow | R ^{2D} \uparrow | F ^{2D} \uparrow | IS ^{3D} \uparrow | FID ^{3D} \downarrow | KID ^{3D} \downarrow | P ^{3D} \uparrow | R ^{3D} \uparrow | F ^{3D} \uparrow |
| DynamicCity[†] [50] | 11 | 1.008 | 7.792 | 8e-3 | 0.108 | 0.009 | 0.017 | 1.269 | 1890 | 0.369 | 0.028 | - | - |
| UniScene [18] | | 1.015 | 0.728 | 5e-4 | 0.295 | 0.572 | 0.389 | 1.278 | 495.6 | 0.027 | 0.387 | 0.482 | 0.429 |
| \mathcal{X}-Scene (Ours) | | 1.030 | 0.275 | 6e-5 | 0.744 | 0.772 | 0.757 | 1.287 | 281.3 | 0.009 | 0.766 | 0.785 | 0.775 |
| UniScene [18] | 17 | 1.023 | 0.770 | 6e-4 | 0.259 | 0.588 | 0.360 | 1.235 | 529.6 | 0.024 | 0.382 | 0.412 | 0.396 |
| \mathcal{X}-Scene (Ours) | | 1.028 | 0.262 | 6e-5 | 0.762 | 0.811 | 0.785 | 1.276 | 258.8 | 0.004 | 0.769 | 0.787 | 0.778 |

User-Prompted Generation and Editing. The lower part of Figure 4 demonstrates the flexibility of \mathcal{X} -Scene in interactive scene generation, supporting both user-prompted generation and geometric editing. Users can provide high-level prompts (e.g., "create a busy intersection"), which are processed to generate corresponding layouts and scene content. Furthermore, given an existing scene, users can specify editing intents (e.g., "remove the parked car") or adjust low-level geometric attributes. Our pipeline updates the scene graph accordingly and regenerates the scene through conditional diffusion.

4.3 Main Result Comparisons

Occupancy Reconstruction and Generation. Table 1 presents the comparative occupancy reconstruction results. The results show that \mathcal{X} -Scene achieves superior reconstruction performance, significantly outperforming prior approaches under similar compression settings (e.g., +0.8% mIoU and +2.5% IoU compared to UniScene [18]). This improvement is attributed to the enhanced capacity of our triplane representation to preserve geometric details while maintaining encoding efficiency.

Table 2 presents the quantitative results for 3D occupancy generation. Following the protocol in [50], we report performance under two settings: (1) a label-mapped setting, where 11 classes are evaluated by merging similar categories (e.g., car, bus, truck) into a unified "vehicle" class, and (2) the full

Table 3: **Comparisons of Multi-view Image Generation.** We report FID and evaluate generation fidelity by performing BEV segmentation [81] and 3D object detection [82] tasks on the generated data from the validation set. **Bold** indicates the best, and underline denotes the second-best results.

| Method | Avenue | Synthesis Resolution | FID↓ | BEV Segmentation | | 3D Object Detection | |
|-----------------------------|----------|----------------------|--------------|------------------|----------------|---------------------|--------------|
| | | | | Road mIoU ↑ | Vehicle mIoU ↑ | mAP ↑ | NDS ↑ |
| Original nuScenes [79] | - | - | - | 73.67 | 34.82 | 35.54 | 41.21 |
| BEVGen [35] | RA-L'24 | 224×400 | 25.54 | 50.20 | 5.89 | - | - |
| BEVControl [36] | arXiv'23 | - | 24.85 | 60.80 | 26.80 | - | - |
| DriveDreamer [3] | ECCV'24 | 256×448 | 26.80 | - | - | - | - |
| MagicDrive [1] | ICLR'24 | 224×400 | 16.20 | 61.05 | 27.01 | 12.30 | 23.32 |
| Panacea [5] | CVPR'24 | 256×512 | 16.96 | 55.78 | 22.74 | 11.58 | 22.31 |
| Drive-WM [19] | CVPR'24 | 192×384 | 15.80 | 65.07 | 27.19 | - | - |
| DreamForge [23] | arXiv'25 | 224×400 | 14.61 | 65.27 | 28.36 | 13.01 | 22.16 |
| Glad [14] | ICLR'25 | 256×512 | <u>12.57</u> | - | - | - | - |
| \mathcal{X} -Scene (Ours) | - | 224×400 | 11.29 | 66.48 | 29.76 | 16.28 | 26.26 |
| \mathcal{X} -Scene (Ours) | - | 336×600 | 12.83 | <u>68.66</u> | <u>32.67</u> | <u>24.92</u> | <u>32.48</u> |
| \mathcal{X} -Scene (Ours) | - | 448×800 | 12.77 | 69.06 | 33.27 | 27.65 | 34.48 |

Table 4: **Comparisons of training support** for semantic occupancy prediction (Baseline as CONet [83]). Table 5: **Comparison of training support** for BEV segmentation (Baseline as CVT [81]) and 3D object detection (Baseline as StreamPETR [84] following the setup in [23, 5]).

| Data Source | Input Modality | 3D Occ Pred. | | Data Type | Data Source | 3D Object Detection | | | BEV Segmentation | |
|-------------------------------|----------------|--------------|-------------|-----------|-----------------------------|---------------------|-------------|-------------|-------------------|-------------------|
| | | IoU ↑ | mIoU ↑ | | | mAP ↑ | NDS ↑ | mAoE ↓ | Rd. mIoU ↑ | Veh. mIoU ↑ |
| Ori nuScenes | 2D (Images) | 20.1 | 12.8 | Real | Ori nuScenes | 34.5 | 46.9 | 59.4 | 74.30 | 36.00 |
| +MagicDrive [1] | | 21.8 | 13.9 | | Panacea [5] | 22.5 | 36.1 | 72.7 | - | - |
| +UniScene [18] | | 28.6 | 16.5 | | DreamForge [23] | 26.0 | 41.1 | 62.2 | 67.80-6.50 | 28.60-7.40 |
| + \mathcal{X} -Scene (Ours) | | 29.1 | 17.2 | | \mathcal{X} -Scene (Ours) | 28.2 | 43.4 | 61.0 | 68.41-5.89 | 29.23-6.77 |
| Ori nuScenes | 3D (LiDAR/Occ) | 30.9 | 15.8 | Gen. | Vista [2] | 34.0 | 38.6 | - | 76.62-2.32 | 37.71-1.71 |
| +UniScene [18] | | 33.1 | 19.3 | | MagicDrive [1] | 35.4 | 39.8 | - | 79.56-5.26 | 40.34-4.34 |
| + \mathcal{X} -Scene (Ours) | | 35.8 | 22.6 | | UniScene [18] | 36.5 | 41.2 | - | 81.69-7.39 | 41.62-5.62 |
| Ori nuScenes | | 29.5 | 20.1 | | DreamForge [23] | 36.6 | 49.5 | 52.9 | - | - |
| +UniScene [18] | 2D+3D | 35.4 | 23.9 | Real+Gen | Panacea [5] | 37.1 | 49.2 | 54.2 | - | - |
| + \mathcal{X} -Scene (Ours) | | 37.1 | 26.3 | | \mathcal{X} -Scene (Ours) | 39.9 | 51.6 | 51.2 | 83.37-9.07 | 43.05-7.05 |

17-class setting without label merging. Our approach consistently achieves the best performance across both 2D and 3D metrics. Notably, in the 17-class setting without label mapping, we observe substantial improvements, with FID^{3D} reduced by 51.2% (258.8 vs. 529.6), highlighting our method’s capacity for fine-grained category distinction. Additionally, our method demonstrates strong precision and recall, reflecting its ability to generate diverse yet semantically consistent occupancy.

Image Generation Fidelity. Table 3 presents the results of multi-view image generation, including FID scores and downstream task evaluations. Notably, \mathcal{X} -Scene supports high-resolution image generation with competitive fidelity, which is crucial for downstream tasks like 3D reconstruction. The results show that \mathcal{X} -Scene achieves the best FID, with a 4.91% improvement over the baseline [1], indicating superior visual realism. Moreover, \mathcal{X} -Scene consistently outperforms other methods in BEV segmentation and 3D object detection as resolution increases. For BEV segmentation in particular, performance on generated scenes at 448×800 resolution closely matches that on real data, showcasing \mathcal{X} -Scene’s strong conditional generation aligned with downstream visual applications.

Downstream Tasks Evaluation. We evaluate the effectiveness of generated scene data in supporting downstream model training. Table 4 presents results for 3D semantic occupancy prediction. Fine-tuning with our generated 3D occupancy grids significantly improves baseline performance (+4.9% IoU, +6.8% mIoU), as the generated high-resolution grids provide reliable spatial structures that facilitate refinement. Furthermore, combining 2D and 3D modalities yields the best performance, underscoring the effectiveness of our multimodal alignment. Table 5 presents the results for 3D object detection and BEV segmentation tasks. Our method achieves the best performance among all synthetic data sources, demonstrating the higher fidelity and structural consistency of the generated views. These results highlight the potential of our synthesized images to enhance perception models.

Qualitative Comparisons. Figure 5 presents a comparison of joint voxel-and-image generation. The results show that \mathcal{X} -Scene not only produces more realistic images but also achieves superior cross-modal consistency, ensuring better alignment between 3D structures and 2D appearances.

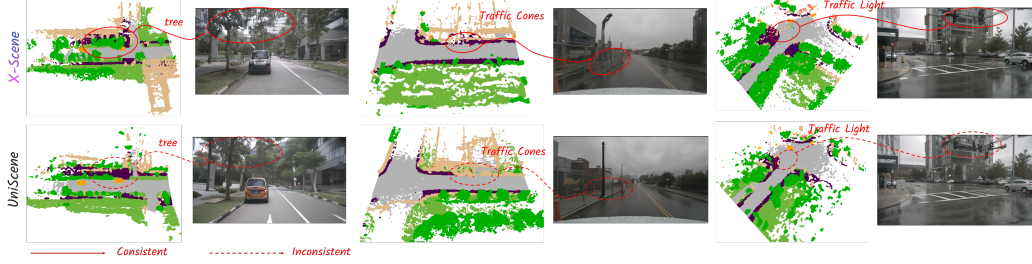


Figure 5: **Qualitative comparison of joint voxel-and-image generation.** Our method achieves superior consistency between generated 3D occupancy and 2D images compared to UniScene [18].

Table 6: **Ablation study** for designs in the occupancy generation model.

| Variants | Triplane Resolution | IoU \uparrow | mIoU \uparrow | FID $^{\text{3D}}\downarrow$ | F $^{\text{3D}}\uparrow$ |
|-----------------------|---------------------|----------------|-----------------|------------------------------|--------------------------|
| <i>X-Scene</i> (Ours) | (100,100,16) | 85.6 | 92.4 | 258.8 | 0.778 |
| w. VAE deformattn | (50,50,16) | 66.6 | 76.6 | 436.1 | 0.522 |
| w/o. VAE deformattn | (50,50,16) | 64.7 | 74.2 | 462.4 | 0.510 |
| w/o. VAE deformattn | (100,100,16) | 84.9 | 91.8 | 266.4 | 0.762 |
| w/o. layout Condition | (100,100,16) | 85.6 | 92.4 | 1584 | 0.237 |
| w/o. box Condition | (100,100,16) | 85.6 | 92.4 | 271.4 | 0.751 |

Table 7: **Ablation study** for designs in the multi-view image generation model.

| Variants | FID | 3D Detection | | | BEV Segmentation | |
|-----------------------|--------------|----------------|----------------|------------------------|------------------------|--|
| | | mAP \uparrow | NDS \uparrow | Rd. mIoU \uparrow | Veh. mIoU \uparrow | |
| <i>X-Scene</i> (Ours) | 11.29 | 16.12 | 26.26 | 66.48 | 29.60 | |
| w/o. semantic map | 12.23 | 15.27 | 25.59 | 65.75 _{-0.73} | 28.71 _{-0.89} | |
| w/o. depth map | 12.94 | 15.61 | 25.98 | 64.87 _{-1.61} | 29.22 _{-0.38} | |
| w/o. perspective map | 16.87 | 13.15 | 22.37 | 63.35 _{-3.13} | 27.13 _{-2.47} | |
| w/o. position embed | 11.38 | 15.60 | 26.16 | 66.46 _{-0.02} | 27.88 _{-1.72} | |
| w/o. text description | 12.60 | 15.54 | 26.06 | 66.26 _{-0.22} | 29.47 _{-0.13} | |

4.4 Ablation Study

Effects of Designs in Occupancy Generation. As shown in Table 6, the proposed triplane deformable attention module improves performance, particularly at lower resolutions. Under the (50, 50, 16) resolution setting, incorporating deformable attention leads to gains of +1.9% in IoU and +2.4% in mIoU, demonstrating its effectiveness in mitigating feature degradation caused by downsampling. We further analyze the impact of different conditioning inputs. Removing either the additive layout condition or the box condition results in reduced generation quality, underscoring their importance in providing fine-grained geometric cues necessary for accurate occupancy field generation.

Effects of Designs in Image Generation. Table 7 presents the ablation results for various conditioning components in the image generation model. Removing the semantic or depth maps that are rendered from 3D occupancy significantly degrades FID and downstream performance, highlighting their importance in providing dense geometric and semantic cues. Excluding the perspective map, which encodes projected 3D boxes and lanes, also reduces downstream performance (with mAP dropping by 2.97%), underscoring its role in conveying explicit layout priors. The 3D positional embedding is particularly critical for object detection, as it enhances localization and spatial representation. Finally, removing the text description degrades generation fidelity (FID worsening by 1.31%), showing that rich linguistic context aids fine-grained appearance modeling and scene understanding.

5 Conclusion and Limitations

In this paper, we present *X-Scene*, a novel framework for 3D driving scene generation that achieves high fidelity, flexible controllability, and large-scale consistency. Through multi-granular control mechanisms, *X-Scene* enables intuitive yet precise scene specification. The joint voxel-and-image generation pipeline ensures detailed geometry and photorealistic appearance, while consistency-aware outpainting preserves spatial coherence in large-scale scenes. Extensive experiments show that *X-Scene* outperforms existing methods in generation quality, controllability, and scalability, making it a powerful tool for driving simulation, data augmentation, and interactive scene exploration. A key limitation of *X-Scene* is its focus on static 3D scene generation. Extending the framework to 4D dynamic scenes generation by modeling moving objects remains an important future direction. Advancing 4D scene generation could further accelerate autonomous driving development by providing high-quality synthetic data and realistic simulation environments for robust training and testing.

χ -Scene: Large-Scale Driving Scene Generation with High Fidelity and Flexible Controllability

Supplementary Material

Contents

| | | |
|----------|---|-----------|
| A | Additional Implementation Details | 11 |
| A.1 | Datasets | 11 |
| A.2 | Model Implementation Details | 11 |
| A.3 | Evaluation Metrics for Occupancy Generation | 12 |
| B | Additional Details of Scene Description Generation | 12 |
| B.1 | Scene Description Memory Construction | 13 |
| B.2 | Novel Scene Description Generation | 13 |
| B.3 | Prompt Details and Scene Description Examples | 14 |
| C | Additional Qualitative Results | 18 |
| C.1 | Conditional Occupancy and Image Generation | 18 |
| C.2 | Text-to-Scene Generation | 22 |
| C.3 | Large-Scale Scene Generation | 22 |
| D | Potential Societal Impact & Limitations | 22 |
| D.1 | Societal Impact | 22 |
| D.2 | Known Limitations | 22 |
| E | Public Resources Used | 23 |
| E.1 | Public Datasets Used | 23 |
| E.2 | Public Implementations Used | 23 |












A Additional Implementation Details

In this section, we provide additional implementation details to facilitate reproducibility. Specifically, we elaborate on the experimental datasets, model implementation, and the evaluation metrics for occupancy generation.

A.1 Datasets

We use Occ3D-nuScenes [78] to train our controllable occupancy generation module, and nuScenes [79] for the multi-view image generation module. Additionally, the textual scene graph-to-layout generation module is trained using 3D bounding box and map annotations from nuScenes. The dataset consists of 700 training scenes and 150 validation scenes, covering diverse environments such as urban areas and industrial zones under various lighting and weather conditions. It includes 17 semantic categories, represented at a resolution of $200 \times 200 \times 16$. Following the setting in DynamicCity [50], we map the original categories to 11 commonly used semantic classes (see Table 8) and conduct experiments both with and without label mapping to enable comprehensive comparisons.

Table 8: **Summary of Semantic Label Mappings.** We map the original 17-class nuScenes semantic labels to 11 classes following the protocol in [50] to enable comprehensive evaluation.

| Mapped Class 11 |  Building |  Barrier |  Free |  Pedestrian |  Pole |  Road |  Ground |  Sidewalk |  Vegetation |  Vehicle |  Bicycle |
|----------------------|--|---|--|--|--|--|--|--|--|---|---|
| Original Class 17 | Manmade | Barrier | Free | Pedestrian | Traffic cone | Driveable surface | Other flat Terrain | Sidewalk | Vegetation | Bus, Car, Const. veh., Trailer, Truck | Bicycle, MotorCycle |

A.2 Model Implementation Details

Textual Scene Description Generation Module. To construct the scene description memory bank \mathcal{M} , we utilize QWen2.5-VL [85] to extract structured information from nuScenes. For each frame, six surround-view images are jointly processed to generate holistic scene descriptions, which are parsed into scene style \mathcal{S} , foreground objects \mathcal{O} , and background elements \mathcal{B} . Concurrently, 3D bounding boxes and lane markings are converted into textual scene-graph layouts \mathcal{L} . These components collectively form memory entries $m_i = \{\mathcal{S}, \mathcal{O}, \mathcal{B}, \mathcal{L}\}$.

For retrieval, text descriptions are encoded using OpenAI’s text-embedding-3-small model and indexed with FAISS to enable efficient similarity search. During inference, given a coarse prompt $\mathcal{T}_{\mathcal{P}}$, we retrieve the top- K relevant entries from \mathcal{M} , which are then combined with the prompt and fed into GPT-4o to generate a detailed and structured scene description \mathcal{D} . Please refer to Sec. B for further details and example illustrations.

Scene-Graph to Layout Generation Module. For the scene-graph to layout generation module, training and evaluation were conducted on a single NVIDIA A6000 GPU with 48GB of memory. We employed a batch size of 128 and trained the model for 400 epochs. The optimization was performed using the AdamW optimizer with an initial learning rate of 1×10^{-4} and a cosine annealing scheduler. To ensure stable training and consistent representation, the 3D bounding boxes were normalized using dataset-specific parameters. Each bounding box b_i was parameterized by its center coordinates (x, y, z) , dimensions (l, w, h) , and yaw angle θ . Following standard practices in 3D object detection, we normalized the box center coordinates to the range $[0, 1]$, applied a logarithmic transformation to the dimensions, and represented the yaw angle using its sine and cosine components. Each graph node was augmented with an 8-dimensional noise vector to enhance robustness during training.

Occupancy Generation Module. For the occupancy generation module, the triplane-VAE encodes the original occupancy field with a resolution of $200 \times 200 \times 16$ into a triplane representation of spatial dimensions $(X_h, Y_h, Z_h) = (100, 100, 16)$ and feature dimension $C_h = 16$, reducing

memory consumption while preserving structural details. The triplane-VAE is trained using the Adam optimizer with an initial learning rate of 1×10^{-3} and a step decay factor of 0.1, over 200 epochs on 4 NVIDIA A6000 GPUs with a batch size of 24 per GPU.

During diffusion, the three orthogonal planes are arranged into a unified square feature map by zero-padding the uncovered corners, forming a tensor $\mathbf{h} \in \mathbb{R}^{X_h+Z_h, Y_h+Z_h, C_h}$. Attention is applied across this tensor to capture inter-plane correlations. The diffusion model is trained from scratch using the AdamW optimizer with an initial learning rate of 1×10^{-4} and a cosine scheduler, over 300 epochs with a batch size of 12 per GPU. For occupancy outpainting, we adopt the RePaint sampling strategy with 5 resampling steps and a jump size of 20.

Multi-view Image Generation Module. We initialize the multi-view image generation module with pretrained Stable Diffusion v2.1 weights, while randomly initializing newly added parameters. The diffusion model is trained on 4 NVIDIA A6000 GPUs with a mini-batch size of 8, using the AdamW optimizer with a learning rate of 8×10^{-5} and a cosine learning rate scheduler over 200 epochs. After initial training at a resolution of 224×400 , we fine-tune the model for an additional 50K iterations at higher resolutions of 448×800 and 336×600 . During inference, we use the UniPC [86] scheduler with 20 steps and a Classifier-Free Guidance (CFG) scale of 1.2 to generate the multi-view images.

A.3 Evaluation Metrics for Occupancy Generation

Following the evaluation protocol of DynamicCity [50], we adopt two complementary strategies to assess the quality of occupancy generation:

- **3D Evaluation:** We train a sparse convolutional autoencoder based on the MinkowskiUNet [87] architecture to extract 3D features from generated occupancy fields. Features from the final down-sampling layer are aggregated via global average pooling and used to compute evaluation metrics using the Torch-Fidelity library [88].
- **2D Evaluation:** We render the 3D occupancy fields into 2D images for image-based evaluation. To ensure fair comparison, we standardize the rendering process across all methods using consistent semantic color mappings and camera parameters. We compute IS, FID, and KID using a standard pretrained InceptionV3 [89] network, and use a VGG-16 [90] model for precision and recall. Both networks are fine-tuned on our semantically color-mapped dataset to ensure domain alignment.

To evaluate the quality and diversity of the generated samples, we adopt the following quantitative metrics for a comprehensive evaluation:

- **Inception Score (IS):** Measures both quality and diversity by computing the KL divergence between the conditional label distribution of each image and the marginal distribution over all images. Higher IS indicates sharper and more diverse samples.
- **Fréchet Inception Distance (FID):** Computes the distance between real and generated sample distributions, modeled as Gaussians in the Inception feature space. Lower FID reflects higher fidelity and realism.
- **Kernel Inception Distance (KID):** Calculates the squared Maximum Mean Discrepancy (MMD) between real and generated features using a polynomial kernel. KID is unbiased and less sensitive to sample size than FID.
- **Precision:** Estimates the proportion of generated samples that lie within the support of the real data, based on a confidence region in feature space.
- **Recall:** Measures how well the generated distribution covers the real data, by checking the proportion of real samples within the support of generated data.
- **F1-Score:** The harmonic mean of precision and recall, reflecting the balance between generation quality and coverage.

B Additional Details of Scene Description Generation

The scene description module constructs textual scene representations by integrating vision-language models (VLMs) and large language models (LLMs). As shown in Algorithm 1, a scene memory bank

Algorithm 1: Textual Scene Description Generation via VLM, LLM, and RAG

Input: User prompt \mathcal{T}_P ; Scene dataset $\mathcal{D}_{\text{scene}}$ **Output:** Structured scene description $\mathcal{D} = \{\mathcal{S}, \mathcal{O}, \mathcal{B}, \mathcal{L}\}$

```
1 Offline Stage: Build Memory Bank  $\mathcal{M}$ 
2 for frame  $f$  in  $\mathcal{D}_{\text{scene}}$  do
3   Load 6 surround-view images  $I_f$  ;
4    $\hat{d}_f \leftarrow \text{VLM}(I_f)$  ; // Generate raw description
5    $\mathcal{S}, \mathcal{O}, \mathcal{B} \leftarrow \text{Parse}(\hat{d}_f)$  ; // Parse style, objects, and background
6    $A_f \leftarrow \text{DataAnnotations}(f)$  ; // Extract spatial annotations
7    $\mathcal{L} \leftarrow \text{LayoutFrom}(A_f)$  ; // Convert annotations to textual layout
8    $m_f \leftarrow \{\mathcal{S}, \mathcal{O}, \mathcal{B}, \mathcal{L}, \hat{d}_f\}$  ; // Assemble memory item
9   Add  $m_f$  to memory bank  $\mathcal{M}$  ;

10 Online Stage: Generate Structured Description  $\mathcal{D}$ 
11  $z_P \leftarrow \text{Embed}(\mathcal{T}_P)$  ; // Embed user prompt
12  $\{z_i\} \leftarrow \text{Embed}(m_i.\text{text})$  for all  $m_i \in \mathcal{M}$  ; // Embed memory entries
13  $\mathcal{M}_K \leftarrow \text{TopK}(z_P, \{z_i\})$  ; // Retrieve top-k relevant memories with RAG
14 Format LLM input using  $\mathcal{T}_P$  and  $\mathcal{M}_K$  ; // Prepare input context
15  $\mathcal{D} \leftarrow \mathcal{G}_{\text{description}}(\mathcal{T}_P, \mathcal{M}_K)$  ; // Generate final description via GPT-4o
```

is first built offline using a VLM. During inference, a RAG pipeline selects the most relevant memory items based on a user’s coarse prompt, enabling the LLM to generate detailed, context-grounded scene descriptions. This framework supports flexible and scalable scene description generation.

B.1 Scene Description Memory Construction

To construct the scene description memory bank \mathcal{M} , we leverage QWen2.5-VL [85] to extract structured scene information from the nuScenes dataset. Specifically, for each annotated timestamp, the six surround-view camera images are fed into the VLM to generate a holistic natural language description of the scene. These descriptions are then parsed into structured components $\{\mathcal{S}, \mathcal{O}, \mathcal{B}\}$, representing scene style (e.g., "a rainy afternoon in an urban area"), foreground objects with spatial and appearance attributes (e.g., "a red sedan parked alongside the walkway"), and background elements (e.g., "high-rise buildings in the distance"). In parallel, we convert nuScenes-provided 3D bounding boxes and lane markings into a textual scene-graph layout \mathcal{L} that captures spatial relationships (e.g., "car A is behind truck B", "pedestrian is on the sidewalk near lane L1"). Together, these components form each memory item m_i .

B.2 Novel Scene Description Generation

During inference, given a user-provided coarse prompt \mathcal{T}_P , we employ GPT-4o as the LLM-based generator $\mathcal{G}_{\text{description}}$ and implement a Retrieval-Augmented Generation (RAG) mechanism to enrich the prompt with relevant memory items. Specifically, both the prompt and the entries in the memory bank \mathcal{M} are embedded using a pre-trained sentence embedding model (i.e., text-embedding-3-small). We then retrieve the top-K most semantically similar descriptions from \mathcal{M} . These retrieved examples serve as contextual references, enabling the LLM to generate a rich and coherent scene description $\mathcal{D} = \{\mathcal{S}, \mathcal{O}, \mathcal{B}, \mathcal{L}\}$ tailored to the user’s input.

This design ensures few-shot generalization, allowing the system to interpret ambiguous or sparse user prompts by grounding them in real-world scene contexts. Furthermore, the memory bank \mathcal{M} is modular and extensible, supporting future inclusion of other datasets with minimal adaptation effort.

B.3 Prompt Details and Scene Description Examples

The following system prompt is defined for **constructing scene description memories**. Given two images capturing the 360-degree surroundings, the VLM is guided to **extract and organize key elements of the driving scene** into a comprehensive representation:

System prompt for scene description memory construction with VLM

Given two panoramic images `<image>FRONT_IMAGE</image>` and `<image>BACK_IMAGE</image>` that encapsulate the surroundings of a vehicle in a 360-degree view, your task is to analyze the driving scene.

Your analysis should include the following core information:

- **Time of the day:** Indicate whether it is `daytime` or `nighttime`.
- **Weather:** Specify if it is `sunny`, `rainy`, `cloudy`, `snowy`, or `foggy`.
- **Surrounding environment:** Classify the environment as `downtown`, `urban expressway`, `suburban`, `rural`, `highway`, `residential`, `industrial`, `nature`, etc.
- **Foreground objects:** Identify objects in the foreground, such as `cars`, `buses`, `trucks`, `pedestrians`, `bicycles`, `motorcycles`, `construction vehicles`, `barriers`, `traffic cones`, `traffic signs/lights`, etc.
- **Background elements:** Describe background elements, including `roads`, `sidewalks`, `pedestrian crossings`, `car parks`, `terrain`, `vegetation`, `buildings`, etc.
- **Road condition:** Characterize the road as an `intersection`, `straight road`, `narrow street`, `wide road`, `pedestrian crossing`, etc.
- **Abstract Description:** Provide a concise summary of the scene, integrating details about `scene features`, `foreground objects`, `background information`, and `road conditions`.

Instruction:

- Each panoramic image consists of three smaller images. The first image covers the `left-front`, `directly in front`, and `right-front` views of the vehicle. The second image includes the `left-rear`, `directly behind`, and `right-rear` views.
- When describing **foreground objects**, clearly detail their unique appearance and location. Specify each object's relative position to the ego vehicle using terms like `front`, `back`, `left`, `right`, etc. Avoid referencing terms like `"first/second image"` or directional phrases such as `"front-left/rear-center view"`. If there are multiple objects of the same type, provide a description for each one.
- For **background elements**, provide descriptions of their notable characteristics.
- Assess the presence of objects from the provided candidate list. If an object exists, describe its attributes briefly. If it does not exist, omit it from your output. You may also include objects not listed in the candidates.

Please format your results as follows:

```
{
  "Time of the day": "xxx",
  "Weather": "xxx",
  "Surrounding environment": "xxx",
  "Foreground objects": [
    {"object1 class": "object1 attributes"},
    ...
  ],
  "Background elements": [
    {"element1 class": "element1 attributes"},
    ...
  ],
  "Road condition": "xxx",
  "Abstract Description": "xxx"
}
```

Example output:

```
{
  "time of the day": "daytime",
  "Weather": "sunny",
  "Surrounding environment": "downtown",
  "Foreground objects": [
    {"car": "blue color"},
    {"truck": "gray color"},
  ],
  "Background elements": [
    {"sidewalk": "narrow"},
    {"building": "white color and tall"}
  ],
  "Road condition": "intersection",
  "Abstract Description": "The scene depicts a sunny day in a downtown area with a blue car, gray truck, and a crouching pedestrian. The narrow sidewalk is lined with a white, tall building."
}
```

The following system prompt is defined for **generating novel scene descriptions**. Given a coarse user prompt, the LLM is guided to retrieve semantically relevant scene descriptions from a structured memory bank. These retrieved references are then used to **enrich, clarify, and ground** the final output, resulting in a coherent and contextually accurate scene description:

System prompt for novel scene description generation with LLM+RAG

You are an **intelligent assistant** for detailed driving scene understanding and generation. Given a **coarse user prompt** and a set of **relevant memory items** retrieved from a structured memory bank, your task is to generate a comprehensive, structured description of the target driving scene.

Input Tokens:

- **<text>USER_PROMPT</text>**: a high-level, possibly ambiguous user query describing a scene, e.g., *"a busy urban street at night"*.
- **<JSON>MEMORY</JSON>**: a collection of scene descriptions in JSON format, semantically retrieved as relevant references to the prompt.

These memory examples should be used to **enhance, clarify, and ground** your final output. Your output must strictly follow the specified JSON structure and provide a **cohesive and concrete** description of the driving scene.

Instructions:

- Leverage relevant entries in **<memory>** to help **expand, clarify, or disambiguate** the user's **<prompt>**.
- When information in the prompt is sparse or vague, **infer plausible details** based on common patterns from similar memory entries.
- Be **specific** in describing the following:
 - Spatial relationships between objects (e.g., beside, ahead, behind)
 - Object attributes (e.g., color, type, behavior)
 - Environmental context (e.g., weather, road type, background elements)
- **Do not directly copy** content from memory items; instead, **synthesize** a new, coherent scene inspired by them.
- **Avoid referencing** the tokens **<prompt>** or **<memory>** in the output.

Expected Output Structure (JSON):

```
{
  "Time of the day": "xxx",
  "Weather": "xxx",
  "Surrounding environment": "xxx",
  "Foreground objects": [
    {"object1": "object1 attributes"},
    ...
  ],
  "Background elements": [
    {"element1": "element1 attributes"},
    ...
  ],
  "Road condition": "xxx",
  "Layout": "xxx",
  "Abstract Description": "xxx"
}
```

Example Output:

```
{
  "Time of the day": "daytime",
  "Weather": "cloudy",
  "Surrounding environment": "urban expressway",
  "Foreground objects": [
    {"truck": "red container truck driving ahead"},
    {"motorcycle": "black motorcycle overtaking from the right"}
  ],
  "Background elements": [
    {"overpass": "grey concrete with visible traffic signs"},
    {"vegetation": "small bushes along the road divider"}
  ],
  "Road condition": "straight road",
  "Layout": "The truck is positioned ahead of the motorcycle and is located on the drivable road. The motorcycle is adjacent to the pedestrian crossing."
  "Abstract Description": "A cloudy daytime scene on an urban expressway, with a red container truck ahead and a black motorcycle overtaking. Concrete overpasses and roadside bushes shape the background."
}
```

Representative examples of the generated scene descriptions, including scene style, foreground objects, background elements, and scene-graph layouts, are presented below:

Scene Description Example



Scene Style:

- **Time of the day:** daytime, with diffused lighting due to cloud cover
- **Weather:** light to moderate rain, as indicated by raindrops on the camera lens and wet pavement
- **Surrounding environment:** urban street flanked by mixed-use buildings and parking areas
- **Road condition:** long, straight, two-lane road with clearly marked crosswalks and lane dividers; visibly slick from rainfall

Foreground Objects:

- **Cars (left side):** a variety of parked vehicles, including a dark pickup truck, compact sedans, SUVs, and so on, aligned parallel along the sidewalk; some cars have reflections on the wet ground
- **Cars (right side):** several vehicles parked curbside in front of commercial buildings, including economy cars to midsize SUVs
- **Pedestrian:** an individual wearing a bright orange reflective safety vest and holding a red umbrella, standing near a crosswalk, suggesting a crossing action in progress
- **Traffic cone:** bright orange cone placed on the sidewalk near the edge of a parking entrance, likely for safety or to reserve space
- **Traffic sign:** a yellow pedestrian crossing sign mounted on a pole; the sign is positioned close to a glass-door building entrance

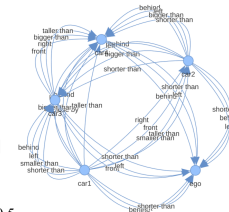
Background Elements:

- **Road:** appears dark and glossy due to recent rainfall; lane markings and crosswalks are clearly visible
- **Sidewalk:** wide, concrete sidewalks run alongside the road, bordered by planters and lined with trees
- **Buildings:** prominent structures include multi-level modern commercial buildings with large glass façades
- **Trees:** scattered urban landscaping includes small trees planted at regular intervals, offering a touch of greenery
- **Car Parking:** multiple designated parking areas, some directly along the street and others within enclosed lots
- **Crosswalk:** wide white-striped pedestrian crossings present at intersections
- **Streetlights:** installed at intervals along the road to provide visibility during low-light conditions

Scene-Graph Layout:

Traffic Light Existing: False

— Crosswalk [(-9.6, -50.1), (-9.4, -43.3), (-12.8, -43.2), (-13.0, -50.0)]
 — Current **straight lane** [(-0.7, -15.0), (-0.5, -8.2), (-0.3, -1.4), (-0.1, +5.4)]
 — ego vehicle **on top of** the lane
 — **Straight lane** with-flow [(-1.5, -45.0), (-1.3, -39.2), (-1.2, -33.4), (-1.0, -27.6)]
 — **vehicle.car** **on top of** the lane, same direction as ego in the **left back**, location: (-1.8, -32.1, +1.1).
 — **Straight lane** allowing from left to right driving [(+6.3, -20.6), (+12.5, -20.5), (+18.7, -20.5), (+24.9, -20.5)]
 — **Straight lane** opposite-flow [(-4.8, -37.9), (-4.7, -41.9), (-5.3, -45.9), (-4.8, -49.9)]
 — Other Lanes/Roadside
 — movable_object.trafficcone in the **left front** location: (-11.4, +9.9, +0.3).length: 0.9, width: 0.4, height: 0.5.
 — movable_object.trafficcone in the **left front** location: (-13.4, +10.0, +0.4).length: 0.4, width: 0.3, height: 0.8.
 — **vehicle.car**.parked in the **left**, heading from left to right, location: (-18.6, -0.1, +0.6).length: 4.2, width: 1.9, height: 1.4.
 — **vehicle.car**.parked in the **left back**, heading from left to right, location: (-18.6, -2.6, +0.9).length: 4.6, width: 2.1, height: 1.8.
 — **vehicle.car**.parked in the **left back**, heading from left to right, location: (-18.4, -5.2, +0.6).length: 4.2, width: 1.9, height: 1.5.
 — **human.pedestrian**.moving in the **right front**, opposite direction, location: (+7.2, +20.0, +1.2).length: 0.9, width: 0.7, height: 1.7.
 — **human.pedestrian**.standing in the **left back**, heading from left to right, location: (-13.2, -30.6, +0.8).length: 0.6, width: 0.6, height: 1.7.
 — **human.pedestrian**.standing in the **left back**, heading from left to right, location: (-13.2, -31.3, +0.9).length: 0.5, width: 0.6, height: 1.7.
 —



Abstract Description:

- The scene shows a rainy day on an urban expressway with wet roads reflecting light. Numerous cars are parked on both sides of the street, and a pedestrian in a bright orange safety vest is near the crosswalk. The background features multi-story commercial buildings with large windows, trees lining the sidewalk, and various signage. Streetlights are visible, and the area is marked with crosswalks and lane lines, creating a realistic and structured urban driving scene.

Scene Description Example



Scene Style:

- **Time of the day:** bright daytime with clear shadows, indicating direct sunlight and good visibility
- **Weather:** sunny with partly cloudy skies; no signs of precipitation or poor visibility
- **Surrounding environment:** suburban campus or business park-like area with a mix of roadways, pedestrian paths, and landscaped
- **Road condition:** smooth asphalt with a gentle curve transitioning into a straight segment

Foreground Objects:

- **Barriers (construction zone):** bright orange modular barriers clearly indicating a temporarily restricted area
- **Truck (construction zone):** a white construction truck with visible text parked adjacent to the barriers
- **Stop sign (construction zone):** standard red octagonal stop sign mounted on a metallic pole, reinforcing right-of-way rules
- **Entrance barrier:** red and white striped boom barrier at two vehicle access points, indicating controlled entry
- **Cars:** silver sedan (parked at curve near the booth); black sedan (alongside silver); dark-colored sedan (moving towards camera, on central lane); red and silver vehicles (visible in side/rear view near building and behind the no-entry sign)
- **Seated pedestrian:** a person is resting on the grassy area near the right side of the road, shaded by trees

Background Elements:

- **Road:** dual-lane road with center markings and white directional arrows
- **Sidewalk:** paved pathways flanked by grass and shrubs on both sides of the road
- **Buildings:** main visible structure is a multi-story white facility with large windows and blue signage
- **Vegetation:** tall green trees forming canopy along both sides of the road, sculpted bushes reinforce the planned landscape design
- **Car Parking:** clearly delineated lot visible on the left, populated with multiple parked cars
- **Traffic Signage:** a “No Entry” (red circle with horizontal white bar) sign prominently displayed at an access control gate

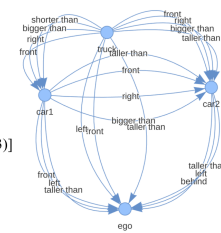
Scene-Graph Layout:

Traffic Light Existing: False

```

|— Current straight lane [(-0.2, -0.6), (-0.1, +2.0), (0.0, +4.6), (+0.1, +7.2)]
|— ego vehicle on top of the lane
|— Straight lane with-flow [(+0.1, +7.2), (+0.2, +10.5), (+0.3, +13.7), (+0.5, +16.9)]
|— movable_object.trafficcone in the left front location: (-1.7, +14.3, +0.6).
|— movable_object.trafficcone in the left front location: (-1.7, +15.0, +0.5).
|— Right turning lane allowing from right to left driving [(+5.9, +50.0), (+5.7, +41.4), (-1.4, +34.9), (-9.8, +34.3)]
|— vehicle.car.moving in the right front, heading from right to left, location: (+0.4, +37.7, +1.3).
|— Left turning lane allowing from left to right driving [(-8.8, +44.4), (-5.3, +45.1), (-1.9, +46.9), (+0.1, +50.0)]
|— vehicle.car.moving in the left back, same direction as ego, location: (-1.2, -29.3, +0.8).
|— Other Lanes/Roadside
|— movable_object.barrier in the left front location: (-2.7, +12.9, +0.7).length: 0.5, width: 2.3, height: 1.2.
|— movable_object.barrier in the left front location: (-3.7, +13.2, +0.8).length: 0.4, width: 2.4, height: 1.2.
|— movable_object.trafficcone in the left front location: (-3.2, +18.8, +0.7).length: 0.3, width: 0.3, height: 0.7.
|— vehicle.bicycle.without_rider in the right front, opposite direction from ego, location: (+9.7, +9.0, +0.2).length: 1.4, width: 0.4, height: 1.1.
|— vehicle.bicycle.without_rider in the right front, opposite direction from ego, location: (+10.3, +8.7, +0.2).length: 1.4, width: 0.5, height: 1.2.
|— vehicle.car.parked in the left front, same direction as ego, location: (-19.3, +4.6, +3.2).length: 4.7, width: 1.9, height: 1.8.
|— vehicle.truck.parked in the left front, heading from left to right, location: (-6.4, +14.5, +2.0).length: 6.5, width: 2.3, height: 3.3.
|— human.pedestrian.adult.sitting_lying_down in the right front, heading from right to left, location: (+9.9, +10.9, +0.2).
|— human.pedestrian.adult.sitting_lying_down in the right front, heading from right to left, location: (+9.5, +11.7, +0.3).
|— .....

```



Abstract Description:

- The scene shows a sunny day in a suburban area with a mix of urban infrastructure and greenery. The road curves slightly before straightening out, with construction barriers and a stop sign indicating ongoing work. Several cars are parked along the roadside, while others are in motion. A pedestrian is seated on the grass near the right-rear view, and there are trees and buildings in the background. The road appears well-maintained, with clear lane markings and a mix of open spaces and developed areas.

C Additional Qualitative Results

C.1 Conditional Occupancy and Image Generation

Figure 6 presents additional conditional generation results, where layout conditions are used to synthesize multi-view images and 3D occupancy. These results demonstrate the effectiveness of our approach in generating coherent multi-modal outputs conditioned on low-level layout inputs.

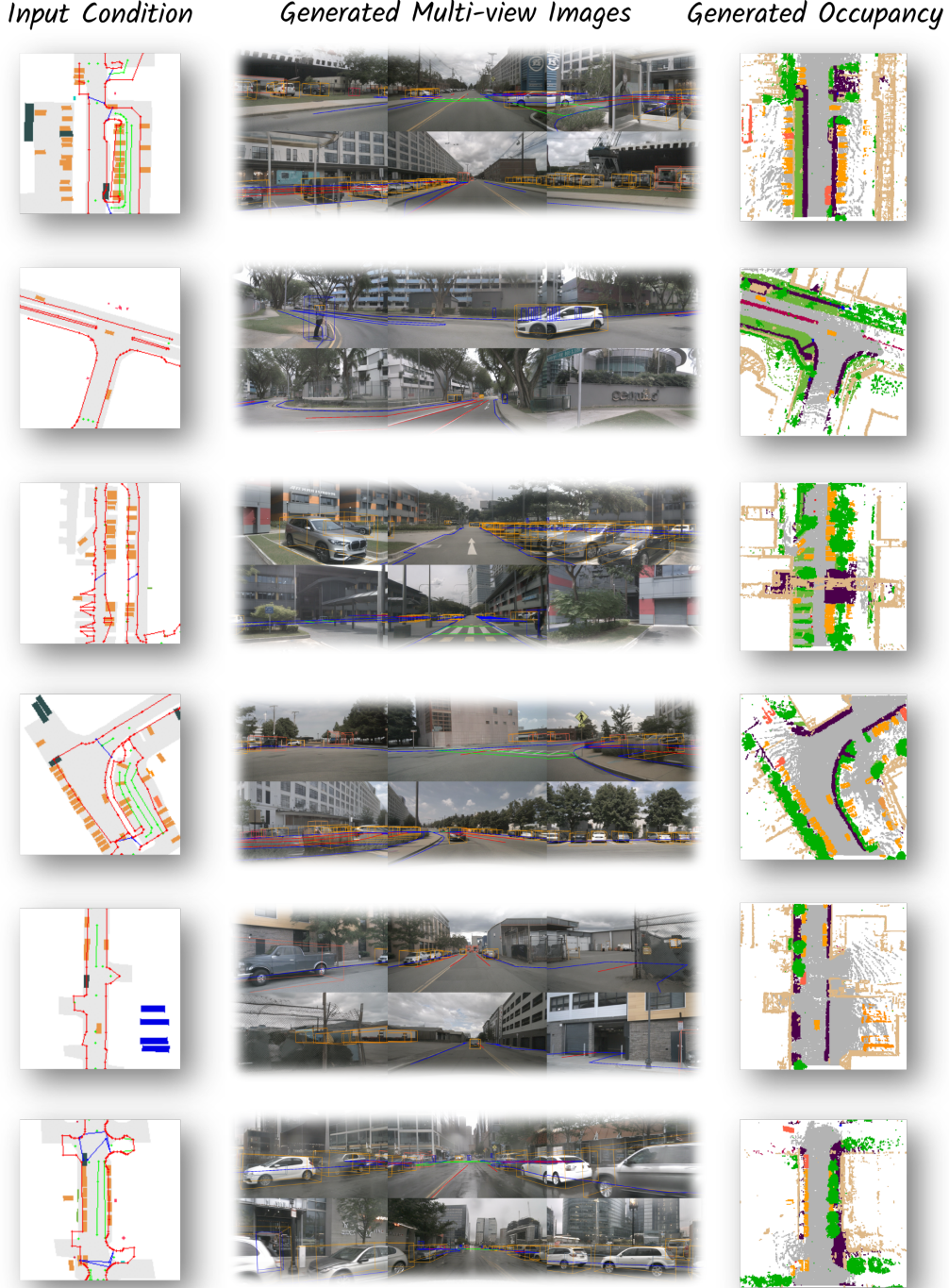
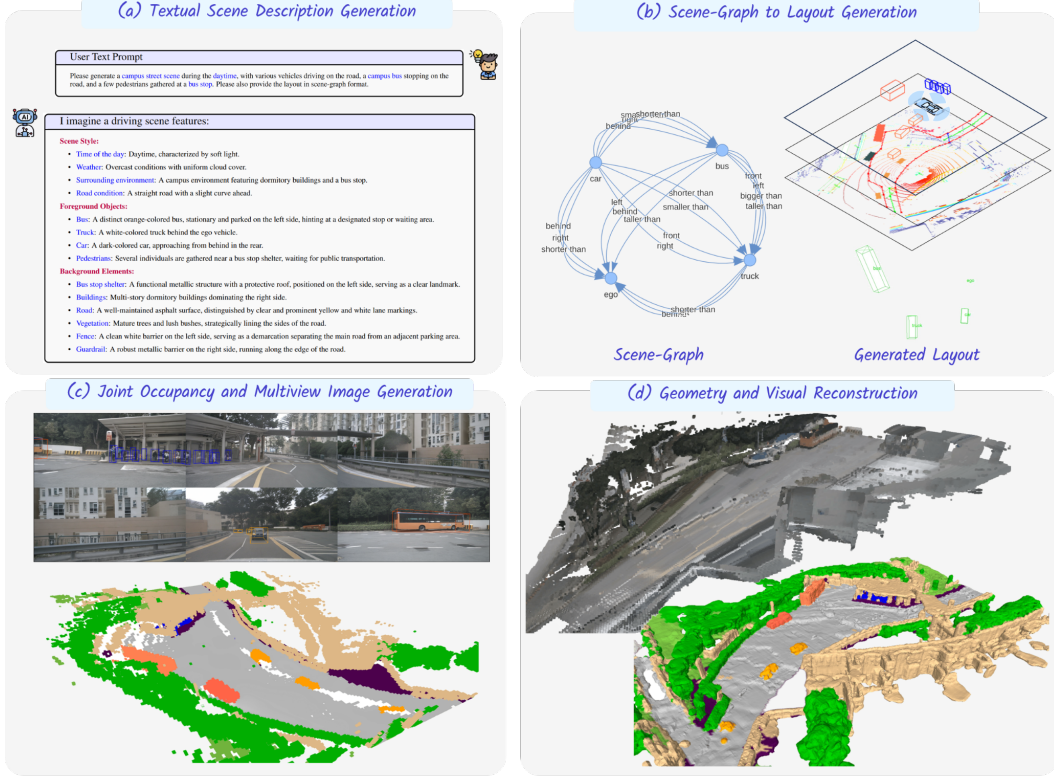
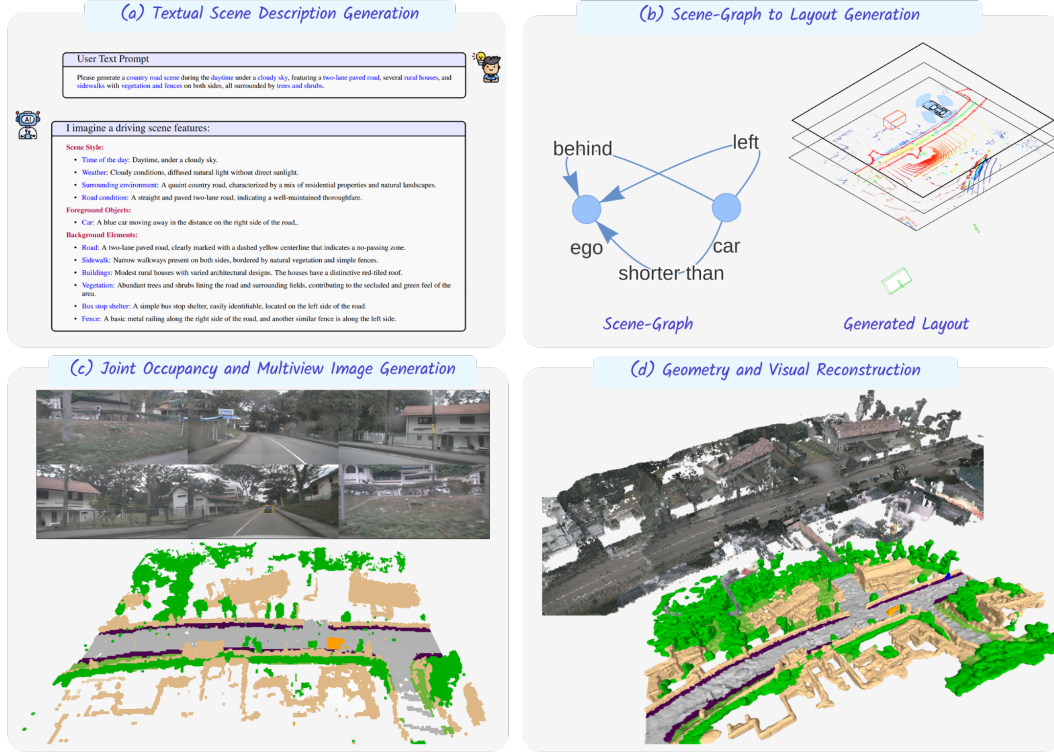


Figure 6: **Additional qualitative results of χ -Scene on conditional occupancy and image generation.** These results demonstrate the model’s ability to generate semantically consistent and structurally accurate multi-modal outputs conditioned on layout inputs across diverse urban scenes.

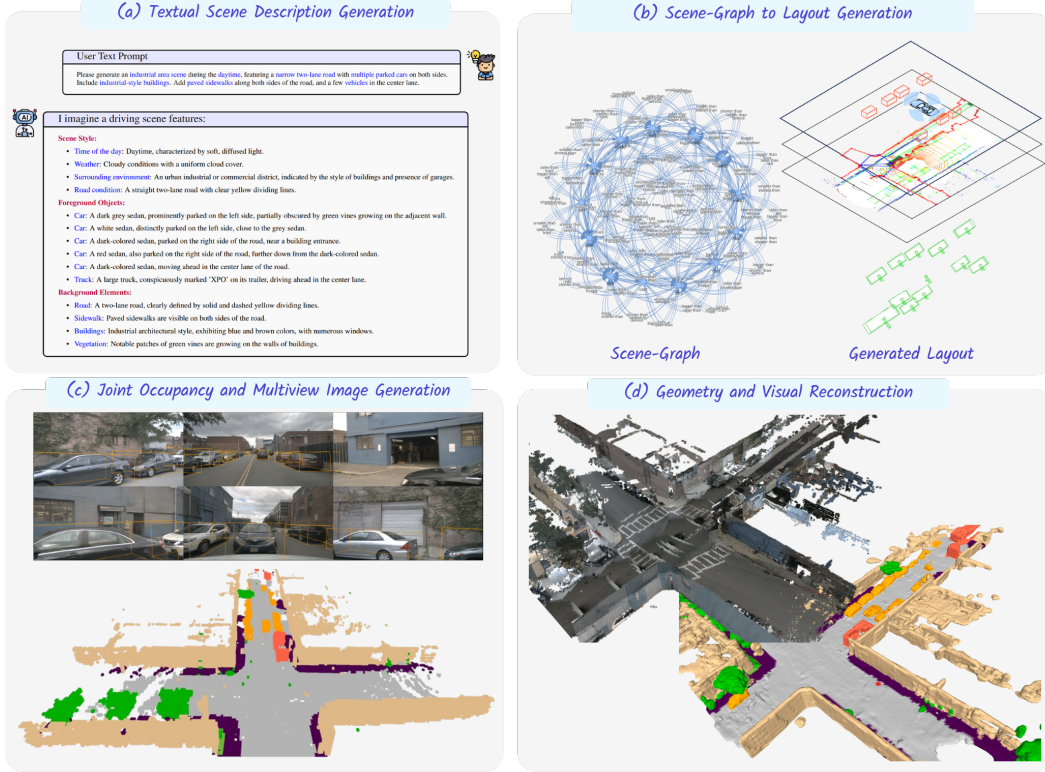


(a) Text-to-Scene Generation Example: Campus Street Scene

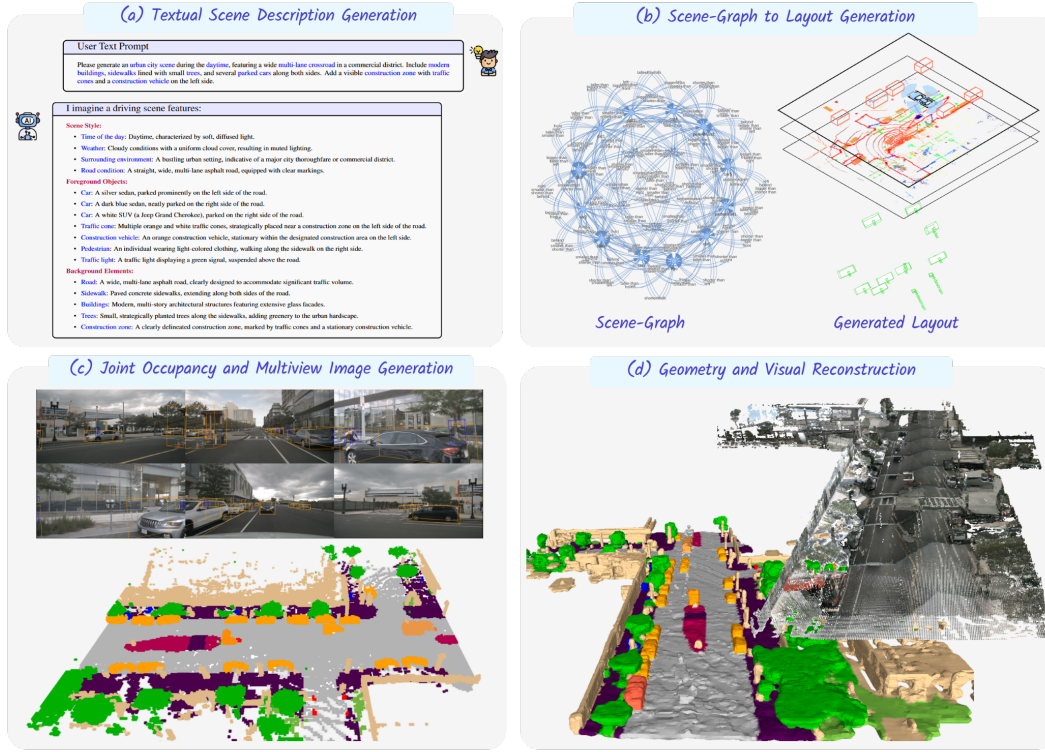


(b) Text-to-Scene Generation Example: Country Road Scene

Figure 7: **Qualitative results of the text-to-scene generation pipeline of \mathcal{X} -Scene**. Starting from a user prompt, the system generates a plausible scene description, constructs the corresponding layout, synthesizes consistent occupancy and multi-view images, and finally performs 3D reconstruction.



(c) Text-to-Scene Generation Example: Industrial Narrow Road Scene



(d) Text-to-Scene Generation Example: City Crossroad Scene

Figure 8: **Qualitative results of the text-to-scene generation pipeline of \mathcal{X} -Scene.** Starting from a user prompt, the system generates a plausible scene description, constructs the corresponding layout, synthesizes consistent occupancy and multi-view images, and finally performs 3D reconstruction.

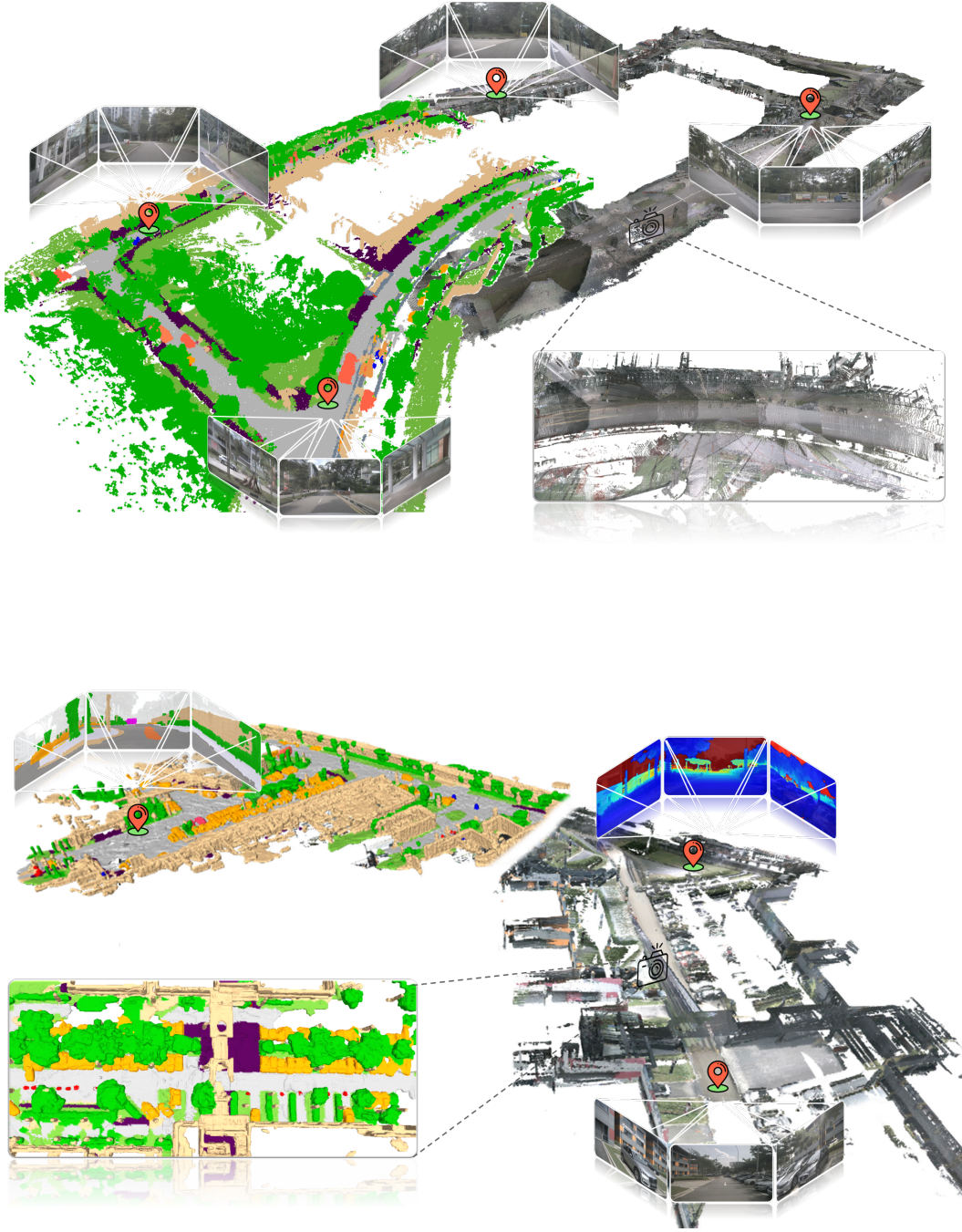


Figure 9: **Qualitative results of large-scale scene generation by \mathcal{X} -Scene**. The model extrapolates coherent occupancy fields and multi-view images across extended areas, enabling high-fidelity and complete 3D scene reconstruction. The generated scenes support novel view synthesis of RGB, depth, and occupancy, demonstrating both geometric consistency and high photorealistic quality at scale.

C.2 Text-to-Scene Generation

Figure 7 and Figure 8 illustrate examples of the text-to-scene generation pipeline, which primarily consists of four steps:

- **Textual scene description generation:** Given a coarse user text prompt, the LLM leverages RAG to retrieve semantically relevant scene descriptions from the memory bank, then composes a plausible scene description encompassing scene style, foreground and background elements, and a textual scene-graph layout.
- **Scene-graph to layout generation:** The layout diffusion model uses the textual scene-graph to generate the corresponding layout, including object bounding boxes and lane lines.
- **Joint occupancy and multi-view image generation:** The occupancy and image diffusion models leverage the layout for geometry control and the text description for semantic control, generating a coherent and realistic 3D occupancy field and multi-view images.
- **Geometry and visual reconstruction:** Given the generated voxels and images, we reconstruct the 3D scene while preserving intricate geometry and realistic appearance, supporting various downstream applications.

These results demonstrate that the proposed text-to-scene pipeline is an effective and flexible method for driving scene generation.

C.3 Large-Scale Scene Generation

Figure 9 illustrates the results of large-scale scene generation. The results show that our method can generate coherent, large-scale driving scenes through consistency-aware extrapolation. Moreover, the generated occupancy and images are fused and lifted for large-scale scene reconstruction, preserving both intricate geometry and realistic visual appearance. The reconstructed scenes support novel RGB, depth, and occupancy rendering.

D Potential Societal Impact & Limitations

In this section, we discuss the potential societal impact of our work and outline its possible limitations.

D.1 Societal Impact

Our proposed framework, \mathcal{X} -Scene, for large-scale controllable driving scene generation holds significant potential for real-world societal impact. By unifying fine-grained geometric accuracy with photorealistic visual fidelity, \mathcal{X} -Scene enables the generation of highly realistic and semantically consistent 3D driving environments. This capability directly supports the development of safer and more efficient autonomous driving systems by enabling rigorous simulation and validation across richly diverse scenarios, including rare cases such as complex intersections, unexpected pedestrian behavior, and unusual road layouts. As a result, \mathcal{X} -Scene can accelerate the development cycle of autonomous vehicles, reduce reliance on costly and time-consuming real-world data collection, and improve safety standards, ultimately contributing to a reduction in traffic-related accidents and fatalities.

D.2 Known Limitations

While \mathcal{X} -Scene offers a promising framework for large-scale controllable 3D scene generation, several limitations remain and warrant further investigation.

First, the current framework is restricted to static 3D scene synthesis and does not account for temporal dynamics. Consequently, it cannot simulate moving objects or evolving scene contexts, which are critical for faithfully modeling real-world driving scenarios. Extending \mathcal{X} -Scene to support dynamic 4D scene generation would allow for more realistic simulations, enabling robust validation of motion forecasting and planning algorithms.

Second, the scene description memory bank is currently built from the nuScenes dataset [79]. While this dataset provides a solid foundation, its limited geometric and semantic diversity may restrict the

range and realism of generated scenes. Incorporating additional datasets featuring a broader range of environments, weather conditions, and traffic patterns would enhance the system’s generalization and scene richness.

Third, the occupancy generation pipeline depends on a fixed set of semantic categories predefined in the training data. As a result, introducing new object types or unseen classes requires retraining the model. This rigidity hinders adaptability in evolving or open-world settings. Future work could explore more extensible architectures that support incremental learning or open-vocabulary generation.

Addressing these limitations is essential for enhancing the realism, scalability, and applicability of \mathcal{X} -Scene in real-world simulation and data generation tasks.

E Public Resources Used

In this section, we acknowledge the public resources used, during the course of this work.

E.1 Public Datasets Used

- nuScenes¹ CC BY-NC-SA 4.0
- nuScenes-devkit² Apache License 2.0
- Occ3D³ MIT License

E.2 Public Implementations Used

- MagicDrive⁴ Apache License 2.0
- SemCity⁵ MIT License
- DynamicCity⁶ Unknown
- DriveArena⁷ Apache License 2.0
- OccSora⁸ Apache License 2.0
- X-Drive⁹ Apache License 2.0
- MinkowskiEngine¹⁰ MIT License
- Torch-Fidelity¹¹ Apache License 2.0
- Qwen2.5-VL¹² Apache License 2.0
- UniScene¹³ Apache License 2.0

¹<https://www.nuscenes.org/nuscenes>

²<https://github.com/nutonomy/nuscenes-devkit>

³<https://tsinghua-mars-lab.github.io/Occ3D>

⁴<https://github.com/cure-lab/MagicDrive>

⁵<https://github.com/zoomin-lee/SemCity>

⁶<https://github.com/3DTopia/DynamicCity>

⁷<https://github.com/PJLab-ADG/DriveArena>

⁸<https://github.com/wzzheng/OccSora>

⁹<https://github.com/yichen928/X-Drive>

¹⁰<https://github.com/NVIDIA/MinkowskiEngine>

¹¹<https://github.com/toshas/torch-fidelity>

¹²<https://github.com/QwenLM/Qwen2.5-VL>

¹³<https://github.com/Arlo0o/UniScene-Unified-Occupancy-centric-Driving-Scene-Generation>

References

- [1] Ruiyuan Gao, Kai Chen, Enze Xie, Lanqing Hong, Zhenguo Li, Dit-Yan Yeung, and Qiang Xu. Magicdrive: Street view generation with diverse 3d geometry control. *arXiv preprint arXiv:2310.02601*, 2023.
- [2] Shenyuan Gao, Jiazhi Yang, Li Chen, Kashyap Chitta, Yihang Qiu, Andreas Geiger, Jun Zhang, and Hongyang Li. Vista: A generalizable driving world model with high fidelity and versatile controllability. *arXiv preprint arXiv:2405.17398*, 2024.
- [3] Xiaofeng Wang, Zheng Zhu, Guan Huang, Xinze Chen, Jiagang Zhu, and Jiwen Lu. Drivedreamer: Towards real-world-drive world models for autonomous driving. In *European Conference on Computer Vision*, pages 55–72. Springer, 2024.
- [4] Xiaofan Li, Yifu Zhang, and Xiaoqing Ye. Drivingdiffusion: Layout-guided multi-view driving scenarios video generation with latent diffusion model. In *European Conference on Computer Vision*, pages 469–485. Springer, 2024.
- [5] Yuqing Wen, Yucheng Zhao, Yingfei Liu, Fan Jia, Yanhui Wang, Chong Luo, Chi Zhang, Tiancai Wang, Xiaoyan Sun, and Xiangyu Zhang. Panacea: Panoramic and controllable video generation for autonomous driving. In *Proceedings of the IEEE/CVF Conference on Computer Vision and Pattern Recognition*, pages 6902–6912, 2024.
- [6] Binyuan Huang, Yuqing Wen, Yucheng Zhao, Yaosi Hu, Yingfei Liu, Fan Jia, Weixin Mao, Tiancai Wang, Chi Zhang, Chang Wen Chen, et al. Subjectdrive: Scaling generative data in autonomous driving via subject control. In *Proceedings of the AAAI Conference on Artificial Intelligence*, volume 39, pages 3617–3625, 2025.
- [7] Ruiyuan Gao, Kai Chen, Bo Xiao, Lanqing Hong, Zhenguo Li, and Qiang Xu. Magicdrivedit: High-resolution long video generation for autonomous driving with adaptive control. *arXiv preprint arXiv:2411.13807*, 2024.
- [8] Leheng Li, Weichao Qiu, Yingjie Cai, Xu Yan, Qing Lian, Bingbing Liu, and Ying-Cong Chen. Syntheocc: Synthesize geometric-controlled street view images through 3d semantic mpis. *arXiv preprint arXiv:2410.00337*, 2024.
- [9] Hannan Lu, Xiaohe Wu, Shudong Wang, Xiameng Qin, Xinyu Zhang, Junyu Han, Wangmeng Zuo, and Ji Tao. Seeing beyond views: Multi-view driving scene video generation with holistic attention. *arXiv preprint arXiv:2412.03520*, 2024.
- [10] Wei Wu, Xi Guo, Weixuan Tang, Tingxuan Huang, Chiyu Wang, Dongyue Chen, and Chenjing Ding. Drivescape: Towards high-resolution controllable multi-view driving video generation. *arXiv preprint arXiv:2409.05463*, 2024.
- [11] Junpeng Jiang, Gangyi Hong, Miao Zhang, Hengtong Hu, Kun Zhan, Rui Shao, and Liqiang Nie. Dive: Efficient multi-view driving scenes generation based on video diffusion transformer. *arXiv preprint arXiv:2504.19614*, 2025.
- [12] Rui Chen, Zehuan Wu, Yichen Liu, Yuxin Guo, Jingcheng Ni, Haifeng Xia, and Siyu Xia. Unimlv: Unified framework for multi-view long video generation with comprehensive control capabilities for autonomous driving. *arXiv preprint arXiv:2412.04842*, 2024.
- [13] Yishen Ji, Ziyue Zhu, Zhenxin Zhu, Kaixin Xiong, Ming Lu, Zhiqi Li, Lijun Zhou, Haiyang Sun, Bing Wang, and Tong Lu. Cogen: 3d consistent video generation via adaptive conditioning for autonomous driving. *arXiv preprint arXiv:2503.22231*, 2025.
- [14] Bin Xie, Yingfei Liu, Tiancai Wang, Jiale Cao, and Xiangyu Zhang. Glad: A streaming scene generator for autonomous driving. *arXiv preprint arXiv:2503.00045*, 2025.
- [15] Yichen Xie, Chenfeng Xu, Chensheng Peng, Shuqi Zhao, Nhat Ho, Alexander T Pham, Mingyu Ding, Masayoshi Tomizuka, and Wei Zhan. X-drive: Cross-modality consistent multi-sensor data synthesis for driving scenarios. *arXiv preprint arXiv:2411.01123*, 2024.
- [16] Zehuan Wu, Jingcheng Ni, Xiaodong Wang, Yuxin Guo, Rui Chen, Lewei Lu, Jifeng Dai, and Yuwen Xiong. Holodrive: Holistic 2d-3d multi-modal street scene generation for autonomous driving. *arXiv preprint arXiv:2412.01407*, 2024.
- [17] Jiachen Lu, Ze Huang, Zeyu Yang, Jiahui Zhang, and Li Zhang. Wovogen: World volume-aware diffusion for controllable multi-camera driving scene generation. In *European Conference on Computer Vision*, pages 329–345. Springer, 2024.

- [18] Bohan Li, Jiazhe Guo, Hongsi Liu, Yingshuang Zou, Yikang Ding, Xiwu Chen, Hu Zhu, Feiyang Tan, Chi Zhang, Tiancai Wang, et al. Uniscene: Unified occupancy-centric driving scene generation. *arXiv preprint arXiv:2412.05435*, 2024.
- [19] Yuqi Wang, Jiawei He, Lue Fan, Hongxin Li, Yuntao Chen, and Zhaoxiang Zhang. Driving into the future: Multiview visual forecasting and planning with world model for autonomous driving. In *Proceedings of the IEEE/CVF Conference on Computer Vision and Pattern Recognition*, pages 14749–14759, 2024.
- [20] Enhui Ma, Lijun Zhou, Tao Tang, Zhan Zhang, Dong Han, Junpeng Jiang, Kun Zhan, Peng Jia, Xianpeng Lang, Haiyang Sun, et al. Unleashing generalization of end-to-end autonomous driving with controllable long video generation. *arXiv preprint arXiv:2406.01349*, 2024.
- [21] Yanhao Wu, Haoyang Zhang, Tianwei Lin, Lichao Huang, Shujie Luo, Rui Wu, Congpei Qiu, Wei Ke, and Tong Zhang. Generating multimodal driving scenes via next-scene prediction. *arXiv preprint arXiv:2503.14945*, 2025.
- [22] Xueming Yang, Licheng Wen, Yukai Ma, Jianbiao Mei, Xin Li, Tiantian Wei, Wenjie Lei, Daocheng Fu, Pinlong Cai, Min Dou, et al. Drivearena: A closed-loop generative simulation platform for autonomous driving. *arXiv preprint arXiv:2408.00415*, 2024.
- [23] Jianbiao Mei, Tao Hu, Xueming Yang, Licheng Wen, Yu Yang, Tiantian Wei, Yukai Ma, Min Dou, Botian Shi, and Yong Liu. Dreamforge: Motion-aware autoregressive video generation for multi-view driving scenes. *arXiv preprint arXiv:2409.04003*, 2024.
- [24] Tianyi Yan, Dongming Wu, Wencheng Han, Junpeng Jiang, Xia Zhou, Kun Zhan, Cheng-zhong Xu, and Jianbing Shen. Drivingsphere: Building a high-fidelity 4d world for closed-loop simulation. *arXiv preprint arXiv:2411.11252*, 2024.
- [25] Chaojun Ni, Guosheng Zhao, Xiaofeng Wang, Zheng Zhu, Wenkang Qin, Guan Huang, Chen Liu, Yuyin Chen, Yida Wang, Xueyang Zhang, et al. Recondreamer: Crafting world models for driving scene reconstruction via online restoration. *arXiv preprint arXiv:2411.19548*, 2024.
- [26] Junhao Ge, Zuhong Liu, Longteng Fan, Yifan Jiang, Jiaqi Su, Yiming Li, Zhejun Zhang, and Siheng Chen. Unraveling the effects of synthetic data on end-to-end autonomous driving. *arXiv preprint arXiv:2503.18108*, 2025.
- [27] Lening Wang, Wenzhao Zheng, Dalong Du, Yunpeng Zhang, Yilong Ren, Han Jiang, Zhiyong Cui, Haiyang Yu, Jie Zhou, Jiwen Lu, et al. Stag-1: Towards realistic 4d driving simulation with video generation model. *arXiv preprint arXiv:2412.05280*, 2024.
- [28] Jumin Lee, Sebin Lee, Changho Jo, Woobin Im, Juhyeong Seon, and Sung-Eui Yoon. Semcity: Semantic scene generation with triplane diffusion. In *Proceedings of the IEEE/CVF conference on computer vision and pattern recognition*, pages 28337–28347, 2024.
- [29] Yifan Lu, Xuanchi Ren, Jiawei Yang, Tianchang Shen, Zhangjie Wu, Jun Gao, Yue Wang, Siheng Chen, Mike Chen, Sanja Fidler, et al. Infinicube: Unbounded and controllable dynamic 3d driving scene generation with world-guided video models. *arXiv preprint arXiv:2412.03934*, 2024.
- [30] Bernhard Kerbl, Georgios Kopanas, Thomas Leimkühler, and George Drettakis. 3d gaussian splatting for real-time radiance field rendering. *ACM Trans. Graph.*, 42(4):139–1, 2023.
- [31] Jonathan Ho, Ajay Jain, and Pieter Abbeel. Denoising diffusion probabilistic models. *Advances in neural information processing systems*, 33:6840–6851, 2020.
- [32] Jiaming Song, Chenlin Meng, and Stefano Ermon. Denoising diffusion implicit models. *arXiv preprint arXiv:2010.02502*, 2020.
- [33] Robin Rombach, Andreas Blattmann, Dominik Lorenz, Patrick Esser, and Björn Ommer. High-resolution image synthesis with latent diffusion models. In *Proceedings of the IEEE/CVF conference on computer vision and pattern recognition*, pages 10684–10695, 2022.
- [34] Andreas Blattmann, Robin Rombach, Huan Ling, Tim Dockhorn, Seung Wook Kim, Sanja Fidler, and Karsten Kreis. Align your latents: High-resolution video synthesis with latent diffusion models. In *Proceedings of the IEEE/CVF conference on computer vision and pattern recognition*, pages 22563–22575, 2023.
- [35] Alexander Szwedlow, Runsheng Xu, and Bolei Zhou. Street-view image generation from a bird’s-eye view layout. *IEEE Robotics and Automation Letters*, 2024.

- [36] Kairui Yang, Enhui Ma, Jibin Peng, Qing Guo, Di Lin, and Kaicheng Yu. Bevcontrol: Accurately controlling street-view elements with multi-perspective consistency via bev sketch layout. *arXiv preprint arXiv:2308.01661*, 2023.
- [37] Guosheng Zhao, Xiaofeng Wang, Zheng Zhu, Xinze Chen, Guan Huang, Xiaoyi Bao, and Xingang Wang. Drivedreamer-2: Llm-enhanced world models for diverse driving video generation. In *Proceedings of the AAAI Conference on Artificial Intelligence*, volume 39, pages 10412–10420, 2025.
- [38] Guosheng Zhao, Chaojun Ni, Xiaofeng Wang, Zheng Zhu, Xueyang Zhang, Yida Wang, Guan Huang, Xinze Chen, Boyuan Wang, Youyi Zhang, et al. Drivedreamer4d: World models are effective data machines for 4d driving scene representation. *arXiv preprint arXiv:2410.13571*, 2024.
- [39] Vlas Zyrianov, Xiyue Zhu, and Shenlong Wang. Learning to generate realistic lidar point clouds. In *European Conference on Computer Vision*, pages 17–35. Springer, 2022.
- [40] Martin Hahner, Christos Sakaridis, Mario Bijelic, Felix Heide, Fisher Yu, Dengxin Dai, and Luc Van Gool. Lidar snowfall simulation for robust 3d object detection. In *Proceedings of the IEEE/CVF conference on computer vision and pattern recognition*, pages 16364–16374, 2022.
- [41] Yuwen Xiong, Wei-Chiu Ma, Jingkan Wang, and Raquel Urtasun. Ultralidar: Learning compact representations for lidar completion and generation. *arXiv preprint arXiv:2311.01448*, 2023.
- [42] Haoxi Ran, Vitor Guizilini, and Yue Wang. Towards realistic scene generation with lidar diffusion models. In *Proceedings of the IEEE/CVF Conference on Computer Vision and Pattern Recognition*, pages 14738–14748, 2024.
- [43] Vlas Zyrianov, Henry Che, Zhijian Liu, and Shenlong Wang. Lidardm: Generative lidar simulation in a generated world. *arXiv preprint arXiv:2404.02903*, 2024.
- [44] Qianjiang Hu, Zhimin Zhang, and Wei Hu. Rangeldm: Fast realistic lidar point cloud generation. In *European Conference on Computer Vision*, pages 115–135. Springer, 2024.
- [45] Yuheng Liu, Xinke Li, Xueting Li, Lu Qi, Chongshou Li, and Ming-Hsuan Yang. Pyramid diffusion for fine 3d large scene generation. In *European Conference on Computer Vision*, pages 71–87. Springer, 2024.
- [46] Jumin Lee, Woobin Im, Sebin Lee, and Sung-Eui Yoon. Diffusion probabilistic models for scene-scale 3d categorical data. *arXiv preprint arXiv:2301.00527*, 2023.
- [47] Junge Zhang, Qihang Zhang, Li Zhang, Ramana Rao Kompella, Gaowen Liu, and Bolei Zhou. Urban scene diffusion through semantic occupancy map. *arXiv preprint arXiv:2403.11697*, 2024.
- [48] Xuanchi Ren, Yifan Lu, Hanxue Liang, Zhangjie Wu, Huan Ling, Mike Chen, Sanja Fidler, Francis Williams, and Jiahui Huang. Scube: Instant large-scale scene reconstruction using voxplats. *arXiv preprint arXiv:2410.20030*, 2024.
- [49] Xuanchi Ren, Jiahui Huang, Xiaohui Zeng, Ken Museth, Sanja Fidler, and Francis Williams. Xcube: Large-scale 3d generative modeling using sparse voxel hierarchies. In *Proceedings of the IEEE/CVF conference on computer vision and pattern recognition*, pages 4209–4219, 2024.
- [50] Hengwei Bian, Lingdong Kong, Haozhe Xie, Liang Pan, Yu Qiao, and Ziwei Liu. Dynamiccity: Large-scale lidar generation from dynamic scenes. *arXiv preprint arXiv:2410.18084*, 2024.
- [51] Yunzhi Yan, Haotong Lin, Chenxu Zhou, Weijie Wang, Haiyang Sun, Kun Zhan, Xianpeng Lang, Xiaowei Zhou, and Sida Peng. Street gaussians: Modeling dynamic urban scenes with gaussian splatting. In *European Conference on Computer Vision*, pages 156–173. Springer, 2024.
- [52] Ruiyuan Gao, Kai Chen, Zhihao Li, Lanqing Hong, Zhenguo Li, and Qiang Xu. Magicdrive3d: Controllable 3d generation for any-view rendering in street scenes. *arXiv preprint arXiv:2405.14475*, 2024.
- [53] Jiageng Mao, Boyi Li, Boris Ivanovic, Yuxiao Chen, Yan Wang, Yurong You, Chaowei Xiao, Danfei Xu, Marco Pavone, and Yue Wang. Dreamdrive: Generative 4d scene modeling from street view images. *arXiv preprint arXiv:2501.00601*, 2024.
- [54] Jiawei Yang, Jiahui Huang, Yuxiao Chen, Yan Wang, Boyi Li, Yurong You, Apoorva Sharma, Maximilian Igl, Peter Karkus, Danfei Xu, et al. Storm: Spatio-temporal reconstruction model for large-scale outdoor scenes. *arXiv preprint arXiv:2501.00602*, 2024.
- [55] Yunzhi Yan, Zhen Xu, Haotong Lin, Haian Jin, Haoyu Guo, Yida Wang, Kun Zhan, Xianpeng Lang, Hujun Bao, Xiaowei Zhou, et al. Streetcrafter: Street view synthesis with controllable video diffusion models. *arXiv preprint arXiv:2412.13188*, 2024.

- [56] Jiazhe Guo, Yikang Ding, Xiwu Chen, Shuo Chen, Bohan Li, Yingshuang Zou, Xiaoyang Lyu, Feiyang Tan, Xiaojuan Qi, Zhiheng Li, et al. Dist-4d: Disentangled spatiotemporal diffusion with metric depth for 4d driving scene generation. *arXiv preprint arXiv:2503.15208*, 2025.
- [57] Lunjun Zhang, Yuwen Xiong, Ze Yang, Sergio Casas, Rui Hu, and Raquel Urtasun. Copilot4d: Learning unsupervised world models for autonomous driving via discrete diffusion. *arXiv preprint arXiv:2311.01017*, 2023.
- [58] Zetong Yang, Li Chen, Yanan Sun, and Hongyang Li. Visual point cloud forecasting enables scalable autonomous driving. In *Proceedings of the IEEE/CVF Conference on Computer Vision and Pattern Recognition*, pages 14673–14684, 2024.
- [59] Ben Agro, Quinlan Sykora, Sergio Casas, Thomas Gilles, and Raquel Urtasun. Uno: Unsupervised occupancy fields for perception and forecasting. In *Proceedings of the IEEE/CVF Conference on Computer Vision and Pattern Recognition*, pages 14487–14496, 2024.
- [60] Wenzhao Zheng, Weiliang Chen, Yuanhui Huang, Borui Zhang, Yueqi Duan, and Jiwen Lu. Occworld: Learning a 3d occupancy world model for autonomous driving. In *European conference on computer vision*, pages 55–72. Springer, 2024.
- [61] Lening Wang, Wenzhao Zheng, Yilong Ren, Han Jiang, Zhiyong Cui, Haiyang Yu, and Jiwen Lu. Occsora: 4d occupancy generation models as world simulators for autonomous driving. *arXiv preprint arXiv:2405.20337*, 2024.
- [62] Chen Min, Dawei Zhao, Liang Xiao, Jian Zhao, Xinli Xu, Zheng Zhu, Lei Jin, Jianshu Li, Yulan Guo, Junliang Xing, et al. Driveworld: 4d pre-trained scene understanding via world models for autonomous driving. In *Proceedings of the IEEE/CVF Conference on Computer Vision and Pattern Recognition*, pages 15522–15533, 2024.
- [63] Yu Yang, Jianbiao Mei, Yukai Ma, Siliang Du, Wenqing Chen, Yijie Qian, Yuxiang Feng, and Yong Liu. Driving in the occupancy world: Vision-centric 4d occupancy forecasting and planning via world models for autonomous driving. In *Proceedings of the AAAI Conference on Artificial Intelligence*, volume 39, pages 9327–9335, 2025.
- [64] Songen Gu, Wei Yin, Bu Jin, Xiaoyang Guo, Junming Wang, Haodong Li, Qian Zhang, and Xiaoxiao Long. Dome: Taming diffusion model into high-fidelity controllable occupancy world model. *arXiv preprint arXiv:2410.10429*, 2024.
- [65] Andrew Liu, Richard Tucker, Varun Jampani, Ameesh Makadia, Noah Snaveley, and Angjoo Kanazawa. Infinite nature: Perpetual view generation of natural scenes from a single image. In *Proceedings of the IEEE/CVF International Conference on Computer Vision*, pages 14458–14467, 2021.
- [66] Boyang Deng, Richard Tucker, Zhengqi Li, Leonidas Guibas, Noah Snaveley, and Gordon Wetzstein. Streetscapes: Large-scale consistent street view generation using autoregressive video diffusion. In *ACM SIGGRAPH 2024 Conference Papers*, pages 1–11, 2024.
- [67] Yixun Liang, Xin Yang, Jiantao Lin, Haodong Li, Xiaogang Xu, and Yingcong Chen. Luciddreamer: Towards high-fidelity text-to-3d generation via interval score matching. In *Proceedings of the IEEE/CVF conference on computer vision and pattern recognition*, pages 6517–6526, 2024.
- [68] Hong-Xing Yu, Haoyi Duan, Charles Herrmann, William T Freeman, and Jiajun Wu. Wonderworld: Interactive 3d scene generation from a single image. *arXiv preprint arXiv:2406.09394*, 2024.
- [69] Hong-Xing Yu, Haoyi Duan, Junhwa Hur, Kyle Sargent, Michael Rubinstein, William T Freeman, Forrester Cole, Deqing Sun, Noah Snaveley, Jiajun Wu, et al. Wonderjourney: Going from anywhere to everywhere. In *Proceedings of the IEEE/CVF Conference on Computer Vision and Pattern Recognition*, pages 6658–6667, 2024.
- [70] Mengqi Zhou, Jun Hou, Chuanchen Luo, Yuxi Wang, Zhaoxiang Zhang, and Junran Peng. Scenex: Procedural controllable large-scale scene generation via large-language models. *arXiv e-prints*, pages arXiv–2403, 2024.
- [71] Jie Deng, Wenhao Chai, Junsheng Huang, Zhonghan Zhao, Qixuan Huang, Mingyan Gao, Jianshu Guo, Shengyu Hao, Wenhao Hu, Jenq-Neng Hwang, et al. Citycraft: A real crafter for 3d city generation. *arXiv preprint arXiv:2406.04983*, 2024.
- [72] Shougao Zhang, Mengqi Zhou, Yuxi Wang, Chuanchen Luo, Rongyu Wang, Yiwei Li, Zhaoxiang Zhang, and Junran Peng. Cityx: Controllable procedural content generation for unbounded 3d cities. *arXiv preprint arXiv:2407.17572*, 2024.

- [73] Chieh Hubert Lin, Hsin-Ying Lee, Willi Menapace, Menglei Chai, Aliaksandr Siarohin, Ming-Hsuan Yang, and Sergey Tulyakov. Infinitcity: Infinite-scale city synthesis. In *Proceedings of the IEEE/CVF international conference on computer vision*, pages 22808–22818, 2023.
- [74] Haozhe Xie, Zhaoxi Chen, Fangzhou Hong, and Ziwei Liu. Citydreamer: Compositional generative model of unbounded 3d cities. In *Proceedings of the IEEE/CVF conference on computer vision and pattern recognition*, pages 9666–9675, 2024.
- [75] Haozhe Xie, Zhaoxi Chen, Fangzhou Hong, and Ziwei Liu. Gaussiancity: Generative gaussian splatting for unbounded 3d city generation. *arXiv preprint arXiv:2406.06526*, 2024.
- [76] Eric R Chan, Connor Z Lin, Matthew A Chan, Koki Nagano, Boxiao Pan, Shalini De Mello, Orazio Gallo, Leonidas J Guibas, Jonathan Tremblay, Sameh Khamis, et al. Efficient geometry-aware 3d generative adversarial networks. In *Proceedings of the IEEE/CVF conference on computer vision and pattern recognition*, pages 16123–16133, 2022.
- [77] Zhennan Wu, Yang Li, Han Yan, Taizhang Shang, Weixuan Sun, Senbo Wang, Ruikai Cui, Weizhe Liu, Hiroyuki Sato, Hongdong Li, et al. Blockfusion: Expandable 3d scene generation using latent tri-plane extrapolation. *ACM Transactions on Graphics (TOG)*, 43(4):1–17, 2024.
- [78] Xiaoyu Tian, Tao Jiang, Longfei Yun, Yucheng Mao, Huitong Yang, Yue Wang, Yilun Wang, and Hang Zhao. Occ3d: A large-scale 3d occupancy prediction benchmark for autonomous driving. *Advances in Neural Information Processing Systems*, 36:64318–64330, 2023.
- [79] Holger Caesar, Varun Bankiti, Alex H Lang, Sourabh Vora, Venice Erin Liong, Qiang Xu, Anush Krishnan, Yu Pan, Giancarlo Baldan, and Oscar Beijbom. nuscenes: A multimodal dataset for autonomous driving. In *Proceedings of the IEEE/CVF conference on computer vision and pattern recognition*, pages 11621–11631, 2020.
- [80] Julong Wei, Shanshuai Yuan, Pengfei Li, Qingda Hu, Zhongxue Gan, and Wenchao Ding. Oc-llama: An occupancy-language-action generative world model for autonomous driving. *arXiv preprint arXiv:2409.03272*, 2024.
- [81] Brady Zhou and Philipp Krähenbühl. Cross-view transformers for real-time map-view semantic segmentation. In *Proceedings of the IEEE/CVF conference on computer vision and pattern recognition*, pages 13760–13769, 2022.
- [82] Zhijian Liu, Haotian Tang, Alexander Amini, Xinyu Yang, Huizi Mao, Daniela L Rus, and Song Han. Bevfusion: Multi-task multi-sensor fusion with unified bird’s-eye view representation. In *2023 IEEE international conference on robotics and automation (ICRA)*, pages 2774–2781. IEEE, 2023.
- [83] Xiaofeng Wang, Zheng Zhu, Wenbo Xu, Yunpeng Zhang, Yi Wei, Xu Chi, Yun Ye, Dalong Du, Jiwen Lu, and Xingang Wang. Openoccupancy: A large scale benchmark for surrounding semantic occupancy perception. In *Proceedings of the IEEE/CVF International Conference on Computer Vision*, pages 17850–17859, 2023.
- [84] Shihao Wang, Yingfei Liu, Tiancai Wang, Ying Li, and Xiangyu Zhang. Exploring object-centric temporal modeling for efficient multi-view 3d object detection. In *Proceedings of the IEEE/CVF international conference on computer vision*, pages 3621–3631, 2023.
- [85] Shuai Bai, Keqin Chen, Xuejing Liu, Jialin Wang, Wenbin Ge, Sibor Song, Kai Dang, Peng Wang, Shijie Wang, Jun Tang, et al. Qwen2. 5-vl technical report. *arXiv preprint arXiv:2502.13923*, 2025.
- [86] Wenliang Zhao, Lujia Bai, Yongming Rao, Jie Zhou, and Jiwen Lu. Unipc: A unified predictor-corrector framework for fast sampling of diffusion models. *Advances in Neural Information Processing Systems*, 36:49842–49869, 2023.
- [87] Christopher Choy, JunYoung Gwak, and Silvio Savarese. 4d spatio-temporal convnets: Minkowski convolutional neural networks. In *Proceedings of the IEEE/CVF conference on computer vision and pattern recognition*, pages 3075–3084, 2019.
- [88] Anton Obukhov, Maximilian Seitzer, Po-Wei Wu, Semen Zhydenko, Jonathan Kyl, and Elvis Yu-Jing Lin. High-fidelity performance metrics for generative models in pytorch, 2020. Version: 0.3.0, DOI: 10.5281/zenodo.4957738.
- [89] Christian Szegedy, Vincent Vanhoucke, Sergey Ioffe, Jon Shlens, and Zbigniew Wojna. Rethinking the inception architecture for computer vision. In *Proceedings of the IEEE conference on computer vision and pattern recognition*, pages 2818–2826, 2016.
- [90] Karen Simonyan and Andrew Zisserman. Very deep convolutional networks for large-scale image recognition. *arXiv preprint arXiv:1409.1556*, 2014.